ADF640666 SBI /NORDA

(2)

Use of Hierarchical Stepwise Optimization for the Segmentation of Cloud Features

J. E. Peak
Computer Sciences Corporation
Monterey, CA 93943-5006

Prepared for
Atmospheric Directorate
Monterey, CA 93943-5006

Approved for public release; distribution is unlimited. Naval Oceanographic and Atmospheric Research Laboratory, Stennis Space Center, Mississippi 39529-5004.

ABSTRACT

The Hierarchical Stepwise Optimization algorithm of Beaulieu and Goldberg (1989) is applied to the segmentation of satellite images into meaningful, large-scale cloud features. GOES-W visible imagery is used. Several different forms of the cost function are explored in an attempt to improve the segmentation of the Nov. 15, 1983 case. A new cost function is shown to result in a superior segmentation. Both HSWO versions are tested on six additional cases. A modification to the HSWO approach is suggested for future research.

ACKNOWLEDGMENTS

The author gratefully acknowledges the support of the sponsor, Office of Naval Technology, Code 22, Mr. James Cauffman, Program Element 62435N, for making this effort possible.

TABLE OF CONTENTS

USE OF HIERARCHICAL STEPWISE OPTIMIZATION FOR THE SEGMENTATION OF CLOUD FEATURES

1. Introduction

In Peak (1990a), neural networks were investigated as potential tools for the automated classification of satellite cloud features. An architecture, called CIFRS (Cloud Image Feature Recognition System), was proposed. CIFRS would use several neural networks tailored to the interpretation of different types of cloud features, as well as statistical and knowledge-based components to augment and direct the analysis process.

The encouraging results of the preliminary experiment in Peak (1990a) led to an expanded study using manually-derived large-scale cloud features (Peak, 1990b). Using a series of GOES images, a human expert outlined and classified large-scale cloud features and identified the types of clouds contained in them. Peak (1990b) showed that a neural network could classify these features with high levels of accuracy by using only a crude set of inputs.

Peak (1990b) recognized that a portion of the classification skill in those experiments resulted from the fact that a human expert had already divided the image into meaningful regions for the neural network to classify. The location and shape of those regions turned out to contain important information that could be exploited by the neural networks. For this reason, Peak (1990b) included an initial experiment in image segmentation using the Hierarchical Stepwise Optimization (HSWO) algorithm of Beaulieu and Goldberg (1989). A single image was divided into a set of coarse-resolution, cloudiness-percentage "pixels." The application of HSWO to this image showed enough promise that an expanded study of this approach was recommended (Peak, 1990b). The purpose of this paper is to present the results of this expanded test.

2. Digitized Image Data

The data used in this study are taken from the same GOES-W cases used in Peak (1990b) because the desired segmentation into large-scale cloud regions has already been performed by Mr. R. Fett of NOARL. The images were digitized to 75 dots-per-inch using a Xerox scanner at the W.R. Church Computer Center at the U.S. Naval Postgraduate School. The regions digitized were approximately 8 inches wide by 4.75 inches tall, or 356x600 pixels, yielding nearly 215,000 values per image. Since the HSWO cost function (Peak, 1990b) must be evaluated for each pixel and its adjacent neighbors, the scheme begins with as many cost values as approximately 4 times the number of pixels. Thus, if we were to start with the basic, digitized grayshade values, HSWO would have to calculate, and then find the minimum of, 860,000 cost values. After combining the two pixels with the lowest cost, there would be about 859,996 cost values from which to find the minimum, and so on.

Obviously, the computer resources required for this problem are immense unless we reduce the amount of initial data. In this study, it was decided to average the values over regions of 10 pixels x 10 pixels. Thus, the effective resolution is reduced to 7.5 dots per inch and the region scanned becomes 36x60 pixels; a total of 2160 values per image. This data set is much more manageable, although even this size problem takes about 2 h to complete on the Masscomp 5450.

A total of seven images are segmented in this study. The first image is the same Nov. 15, 1983 image from the preliminary test of Peak (1990b). In the next section, several different segmentations of this image will be performed in an attempt to determine the best cost function to be used for cloud imagery. The six remaining images are those taken every three days beginning with Oct. 1, 1983 and ending with Oct. 16, 1983. These situations contain some very complex cloud regions which should provide a wide range of segmentation problems for the scheme.

3. Cost Function Experiments

The HSWO algorithm is straightforward. For each pixel, a region is assigned. The cost $C_{i,j}$ of combining any region i with one of its adjacent regions j is given by

$$C_{i,j} = \frac{N_i * N_j}{N_i + N_j} (x_i - x_j)^2 \qquad (1)$$

where N_i and N_j are the number of pixels, and x_i and x_j are the average grayshade values, of regions i and j, respectively. The two regions with the minimum cost are combined, and the new region is assigned the weighted average grayshade of the two combined regions. The N-terms in (1) tend to assign the lowest cost to combining two very small regions. A small region being combined into a large region is also given a relatively low cost. The highest cost results from trying to combine two, large regions. The x-term in (1) accounts for the difference in grayshade between the regions; obviously assigning lower costs when the grayshades have similar values.

Before presenting the image segmentation results, the criterion for terminating the HSWO process should be mentioned. As in Beaulieu and Goldberg (1989) and in Peak (1990b), the increase in cost function between iterations is used. First, we assume that, for the large scale of cloud regions we are interested in, there should be a reasonably small number of such features present in the region of interest. We arbitrarily choose not to consider stopping the process when there are more than 20 regions in the image. Thus, even large increases in the cost function are ignored until the algorithm has combined the pixels into 20 separate regions. After that point, we look for a large increase in cost between iterations to indicate the stopping point. Because the minimum cost value sometimes oscillates up and down, there may be an apparently large increase in the minimum cost between iterations that is mostly due to a large decrease in the previous iteration rather than a large increase in the present iteration. In other words, we want to look for a large jump from the minimum cost curve trend rather than from individual values. The approach of using an average or weighted average of previous minimum cost values as a basis for comparison was considered. However, it was found that the cost jump between the cost at the current iteration and the largest of the costs at the two previous iterations was sufficient to define the stopping point. A jump of at least 40% is deemed sufficient in this context (at least for now).

In this section, the focus is exclusively on the Nov. 15, 1983 image (Fig. 1). The major features to be isolated are: 1) a

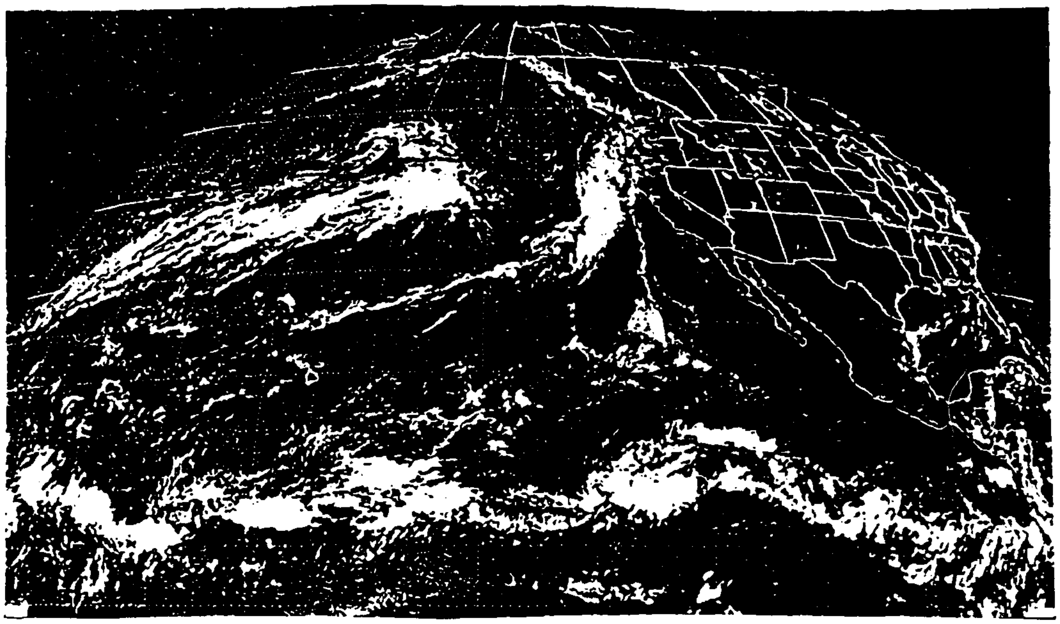

Figure 1. Portion of GOES-W image for Nov. 15, 1983 used for digitization and later segmentation using HSWO.

frontal band in the western, mid-latitudes, 2) a frontal band extending offshore from the Pacific northwest, 3) a region of stratocumulus west of Baja California, and 4) a long, inter-tropical convergence zone (ITCZ) spanning the tropics. There are many smaller-scale features as well, but the focus of this study is to attempt the segmentation of large-scale cloud features only.

The HSWO segmentation of the Nov. 15 case using 7.5 dpi resolution is presented in Fig. 2. All of the image segmentations presented in this paper are in the form of three figures. The first is the image to be segmented with the segmentation regions overlaid in thick, black lines (e.g., Fig. 2a). It was difficult with available photocopiers to get an overlaid segmentation to show up clearly against an image background. For this reason, a figure of the segmentation regions only (e.g., Fig. 2b) is also presented below the overlaid image. The reader should be able to see the segmentation regions clearly in the bottom figure and then look for the corresponding regions in the overlaid figure above. The areas in these figures are labelled by the algorithm during the segmentation process. Thus, the same cloudy area in one segmentation may have a different label in subsequent segmentations. Finally, the minimum cost function values from the last 20 iterations of the segmentation are plotted (e.g., Fig. 2c) including an arrow indicator of the stopping point used. The reader will find that these cost function curves show that the satellite imagery segmentations tend to have the large jumps in minimum cost suggested by Beulieu and Goldberg (1989) as

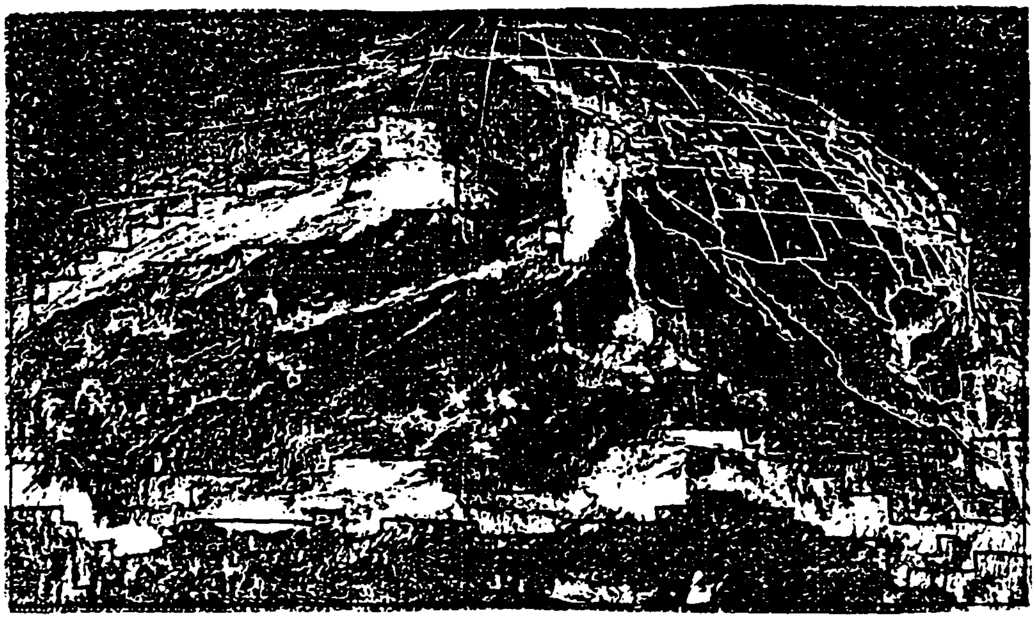

Figure 2a. As in Fig. 1 except after HSWO segmentation. HSWO-defined regions are outlined in heavy, black lines and labeled with numbers or characters.

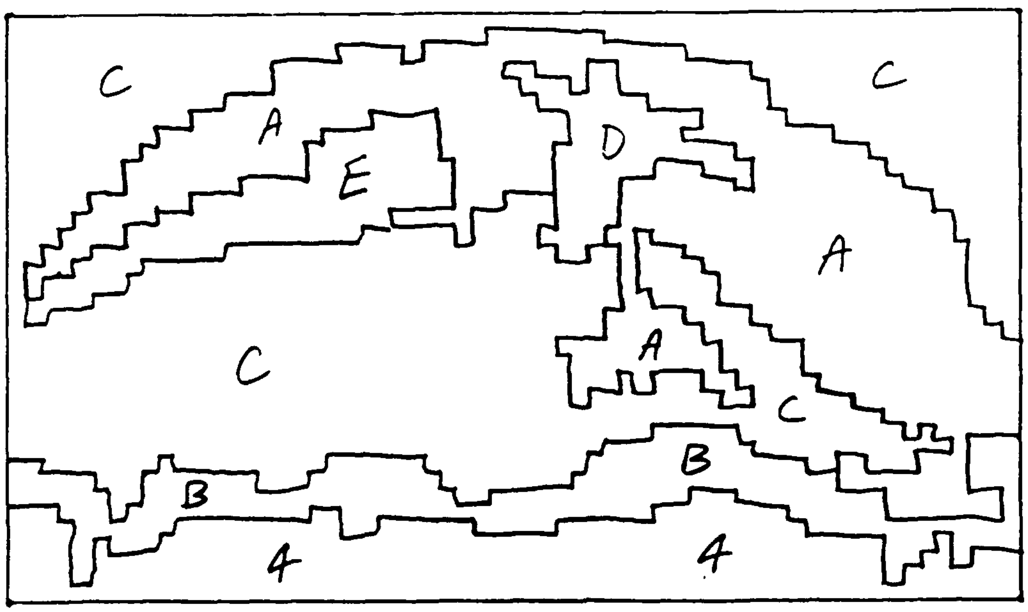

Figure 2b. HSWO segmentation regions that were overlaid on Fig. 2a.

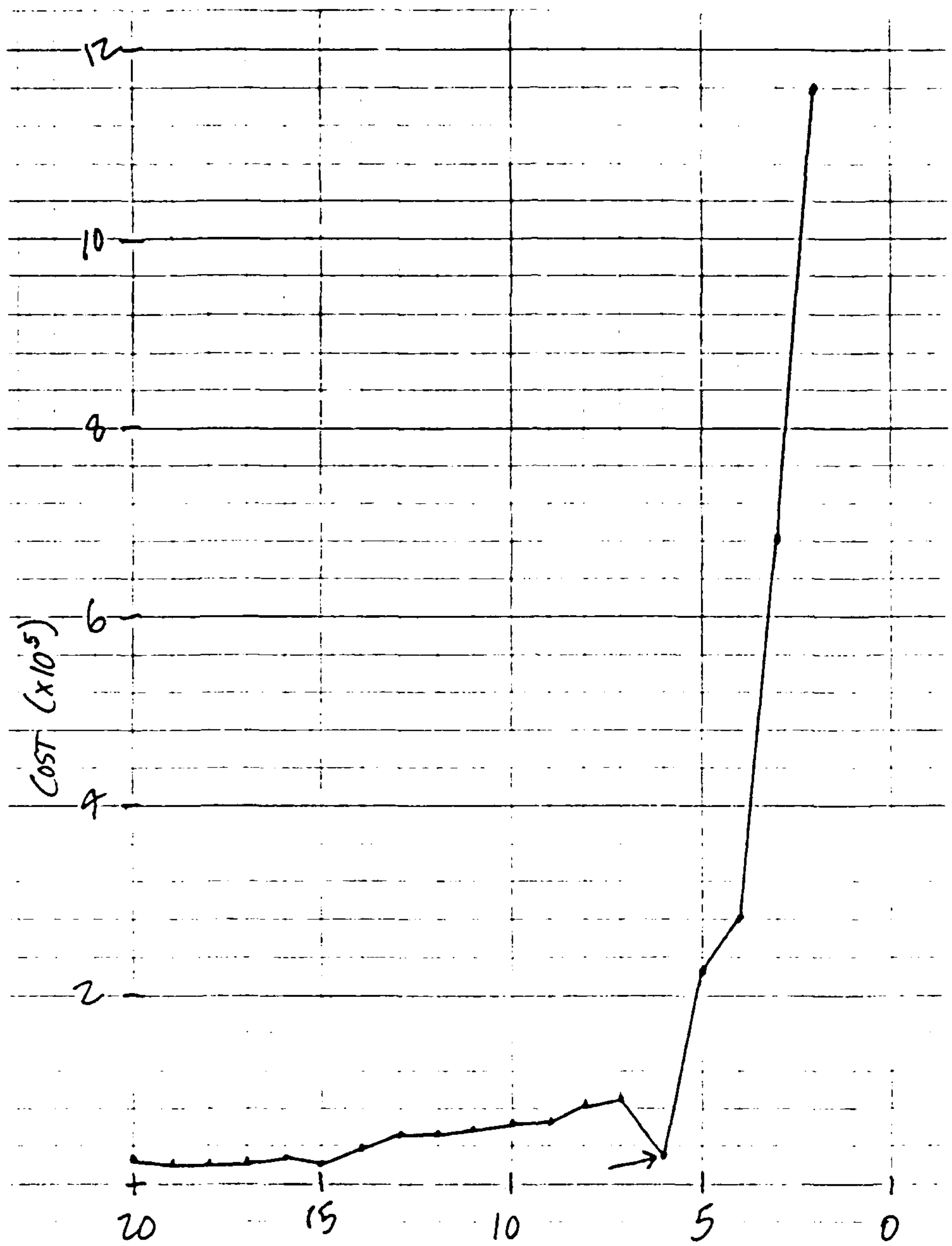

Figure 2c. Minimum cost values as a function of the number of regions left uncombined during the segmentation of the image in Fig. 1. Arrow indicates the cutoff point resulting in the segmentation regions depicted in Fig. 2b.

stopping points.

The segmentation of the Nov. 15 case resulted in six regions (Fig. 2). The minimum cost function curve (Fig. 2c) shows that the minimum cost gradually increases until there are seven regions. At this point, there is a sharp decrease, followed by a large increase. We choose the minimum value at six regions as the stopping point.

The image segmentation (Fig. 2a & b) shows that HSWO does an excellent job of outlining the western front (area E). The main body of the Pacific northwest front (area D) is also segmented well. There is a dim, warm front (that doesn't show up well in these Figures), extending from Washington to northwest Colorado, that is included in area D. One disadvantage in using navigated, photographic images is that the white, coastal lines overlaid on the image tend to contaminate the gray-shade values. For this reason, area D extends to the northwest to include the bright, complex coastline of Alaska and British Columbia. A major disappointment is the failure of HSWO to include the thin, trailing frontal band into area D. This band has instead been incorporated into the mostly noncloudy area C. This region has no meaning in terms of cloud areas; it occurs because the planetary albedo causes it to have some brightness. Interestingly, the planetary portion of C has been included with the outer space background areas at the top left and right of the image. Area 4 is a similar, noncloudy planetary area. Area B indicates that the ITCZ is well-handled by HSWO; it spans the width of the image ignoring local breaks and details in the cloud region.

The stratocumulus region is outlined (area A), but the long, thin cloud band extending to the north has caused HSWO to include it into a broad, dim area that spans the planetary boundary of the image.

For the remainder of this section, attempts to improve on this segmentation will be presented. In particular, we want the routine to be able to discriminate the stratocumulus region and to include the thin, trailing front into the body of the eastern frontal band. The latter problem may be caused by the low resolution of the data. In other words, when the data are reduced to 7.5 dpi, each "pixel" along the thin cloud band will include significant noncloudy information along with the cloudy information. When these data are averaged to 7.5 dpi, the resulting grayshade is artificially low, causing these pixels to be included in the noncloudy region rather than into the body of the front.

To test this hypothesis, a new data set was created by averaging to 15 dpi "pixels." The hope is that HSWO will now have a thin line of smaller, but brighter, pixels to connect to the body of the front. The resulting HSWO segmentation is presented in Fig. 3. The minimum cost function curve (Fig. 3c) indicates that the cutoff should again be at six regions. The resulting segmentation (Fig. 3a & b) again handles the western front (area 8) well. The ITCZ is now broken into two, major regions B and C. Unfortunately, the eastern front (area 9) still does not include the tailing portion. Even with the higher resolution, the average grayshade of the tailing portion is still

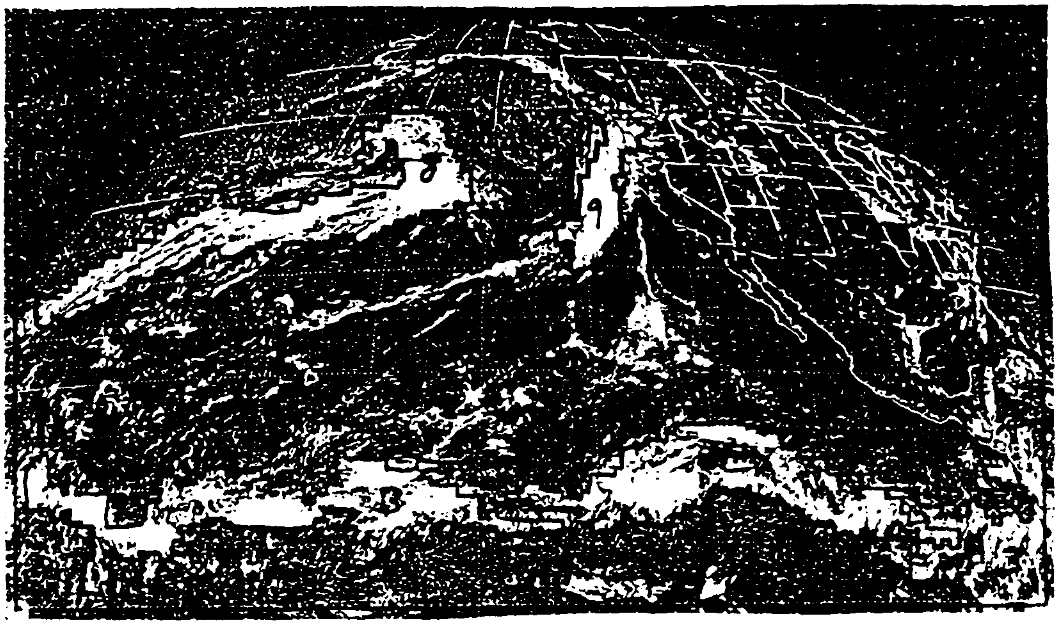

Figure 3a. As in Fig. 2a except for HSWO segmentation using high-resolution data set.

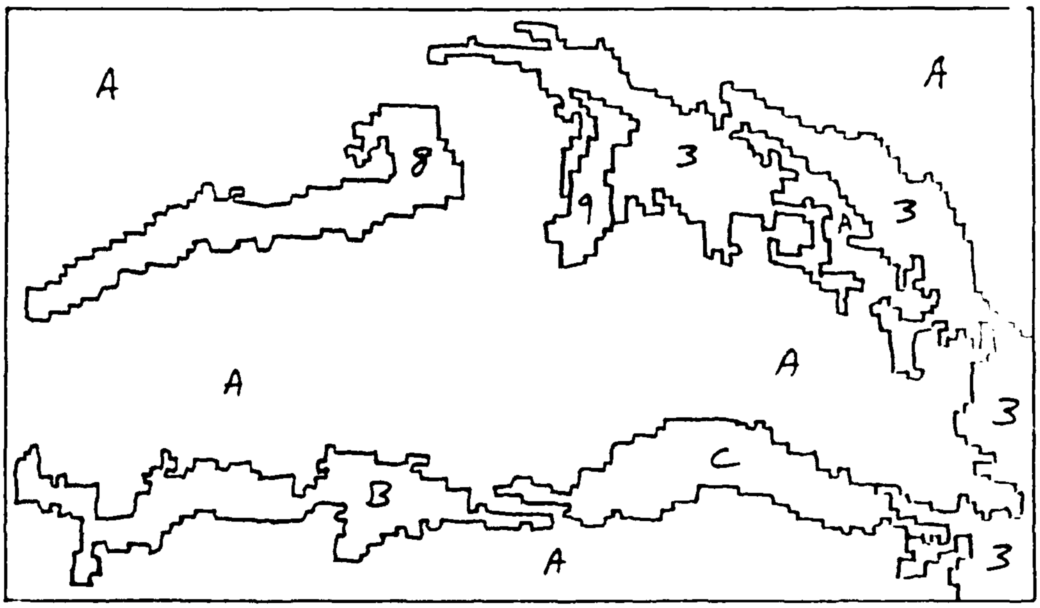

Figure 3b. As in Fig. 2b except for HSWO segmentation using high-resolution data set.

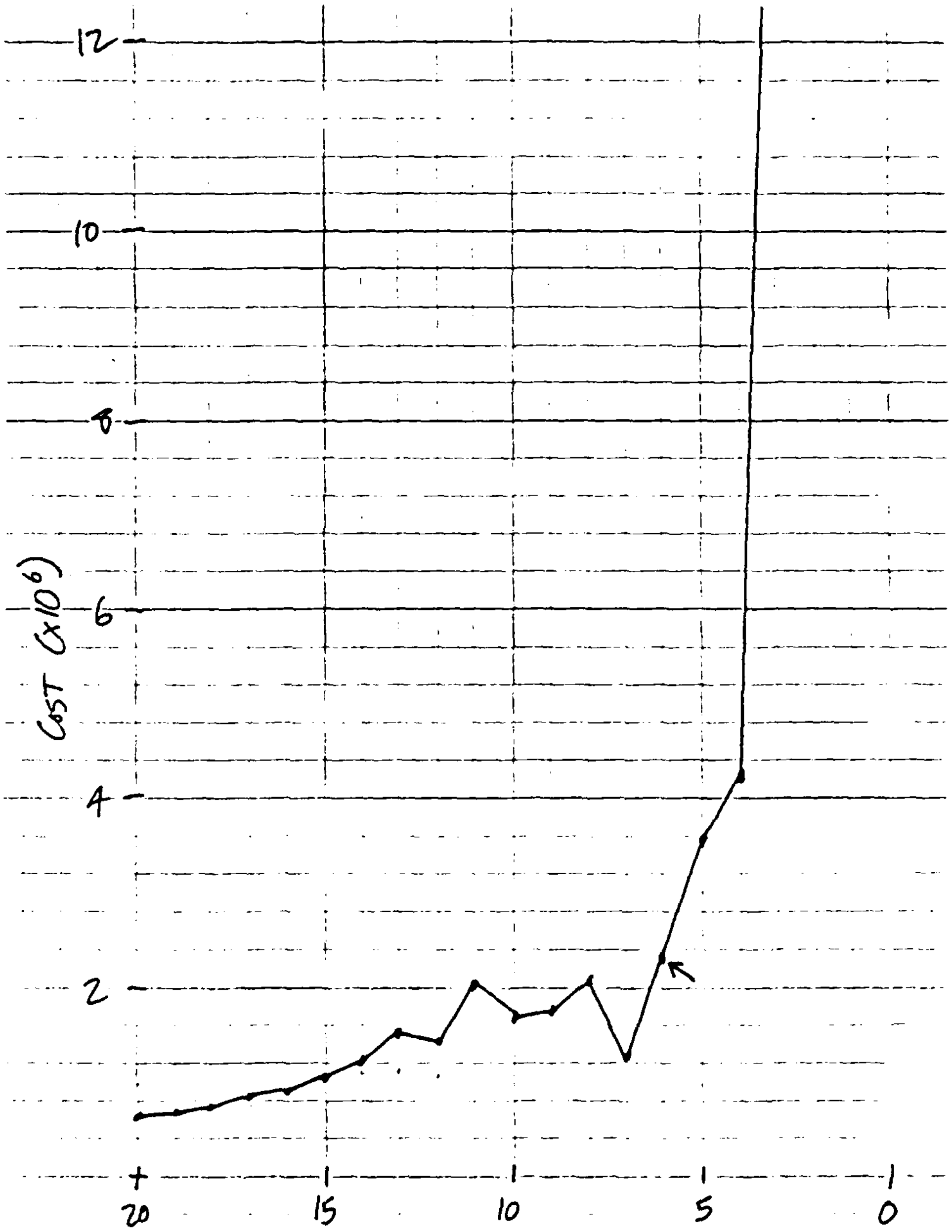

Figure 3c. As in Fig. 2c except for HSWO segmentation using high-resolution data set.

closer to that of the dark background rather than the bright front. Also, the stratocumulus region is now also absorbed into the background region A. It appears that the problem lies in the way that the cost function treats regions with intermediate grayshades. Such regions are susceptible to being joined into adjacent dark regions when their grayshade value is even slightly closer to being dark than bright.

Visiting experts from the National Academy of Sciences suggested that filtering the data before HSWO processing might improve the segmentation. The idea is to decrease the abrupt shift in brightness at region edges to provide a more gradual linking of adjacent, cloudy regions. The Nov. 15 case was filtered using a simple, 9-point filter. The ensuing segmentation is presented in Fig. 4. Again, the western front (area D) is well defined. The ITCZ is now divided into two, separate bands (areas A and E). The eastern front still does not include the trailing front and the stratocumulus region is also combined into the background area B. It appears that the filtering has not accomplished its desired effect, possible because filtering also lowers the grayshade of the intermediate regions, thus making them more susceptible to inclusion in the darker areas.

The nature of the cloud regions we are trying to segment is that any brightness should indicate clouds, and that such regions should almost always be included into adjacent, cloudy regions. Thus, even relatively dim, intermediate regions should be treated as being more like other, brighter regions than as dark regions. To accomplish this behavior, the cost function could be modified.

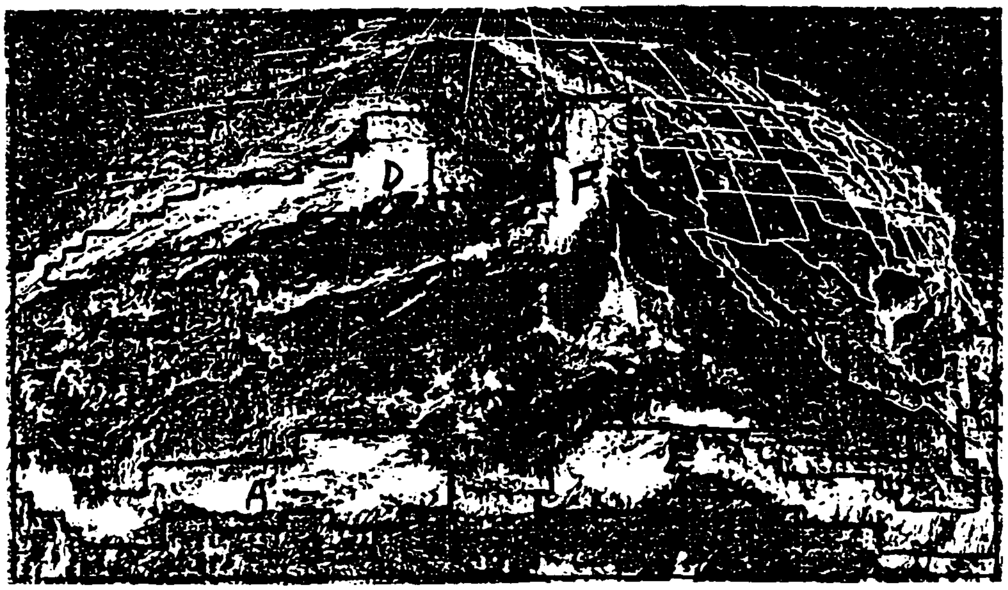

Figure 4a. As in Fig. 2a except for HSWO segmentation using filtered data set.

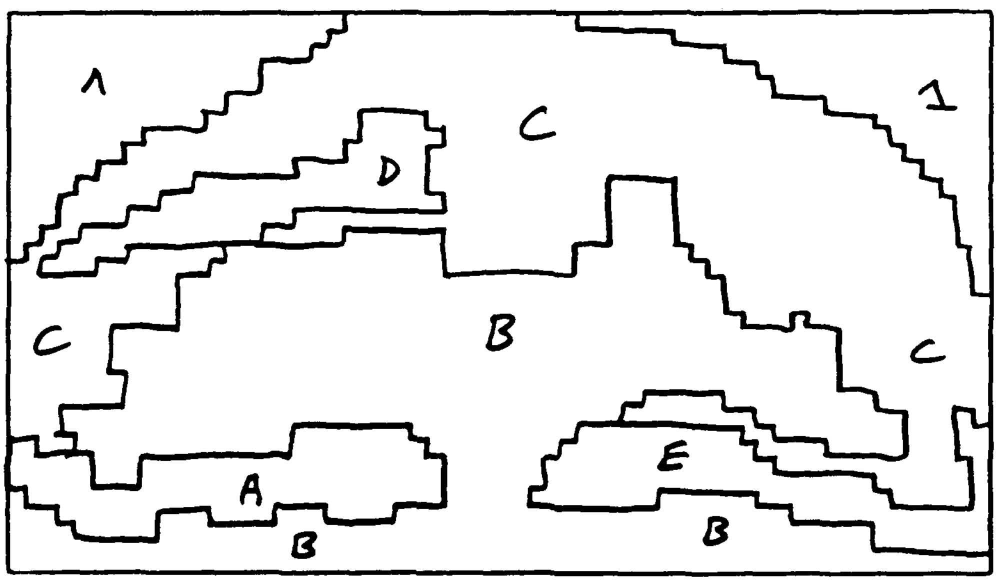

Figure 4b. As in Fig. 2b except for HSWO segmentation using filtered data set.

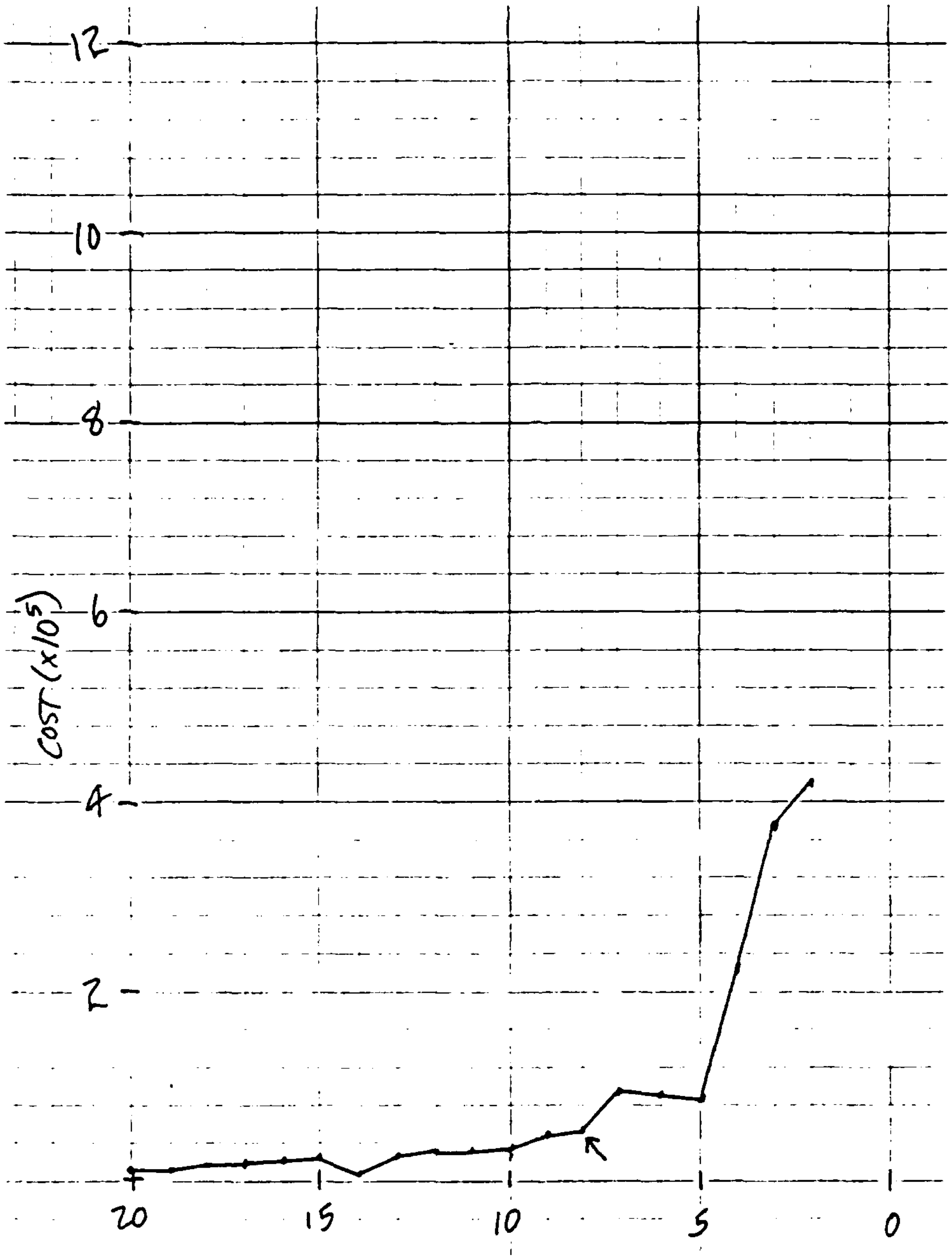

Figure 4c. As in Fig. 2c except for HSWO segmentation using filtered data set.

We choose the new form:

$$C_{i,j} = \frac{N_i * N_j}{N_i + N_j} * \frac{(x_i - x_j)^2}{x_i + x_j} \qquad (2)$$

Here, the grayshade values in the denominator tend to increase the cost when the grayshade of a region is low (close to zero). The goal is to increase the cost of combining a dim, cloudy region with a dark, background region. When both grayshades are low, the grayshade difference in the numerator will be small, thus keeping the cost low for combining dark regions.

The segmentation was rerun using the cost function in (2) (Fig. 5). Notice that there is very little difference between this segmentation and the original (Fig. 5a & b vs. Fig. 2a & b). The only real difference is that the thin cloud band extending northward from the stratocumulus region is now combined with the eastern front (area B) rather than with the background region A. Thus, it may be that the new cost function is having the desired effect, but not to the extent necessary.

To increase the effect of the new cost function, we now square the grayshade term in the denominator:

$$C_{i,j} = \frac{N_i * N_j}{N_i + N_j} * \frac{(x_i - x_j)^2}{(x_i + x_j)^2} \qquad (3)$$

The ensuing segmentation is presented in Fig. 6. As before, the western front (area +) and the ITCZ (area 8) are well-segmented. Notice, however, the added complexity in the regions describing the background (regions A and C) and outer space (regions 1, 3, 6 and [) areas. By squaring the denominator of the grayshade term,

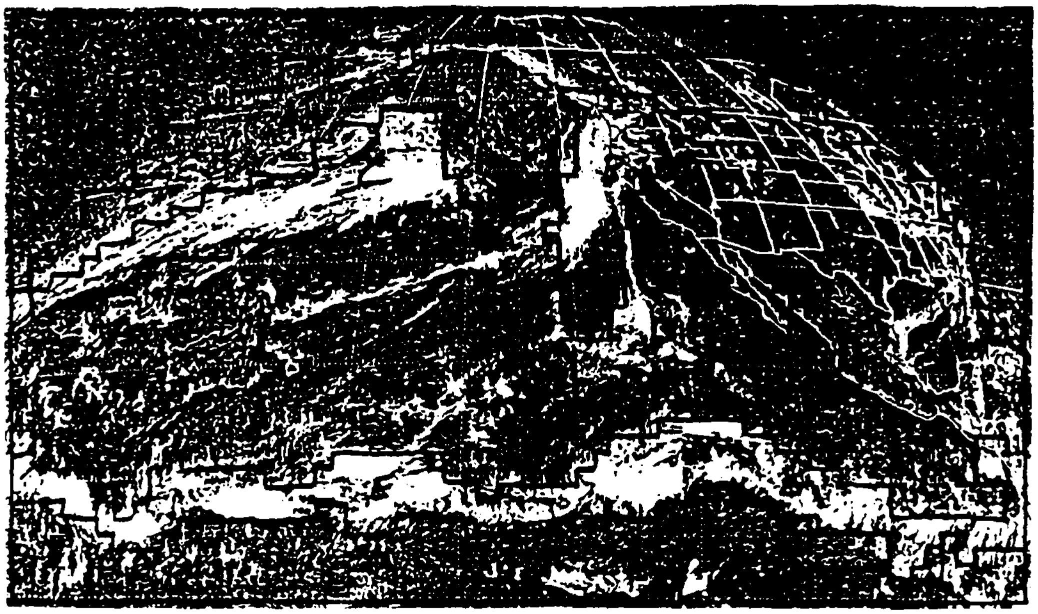

Figure 5a. As in Fig. 2a except for HSWO segmentation using cost function in Eqn. (2).

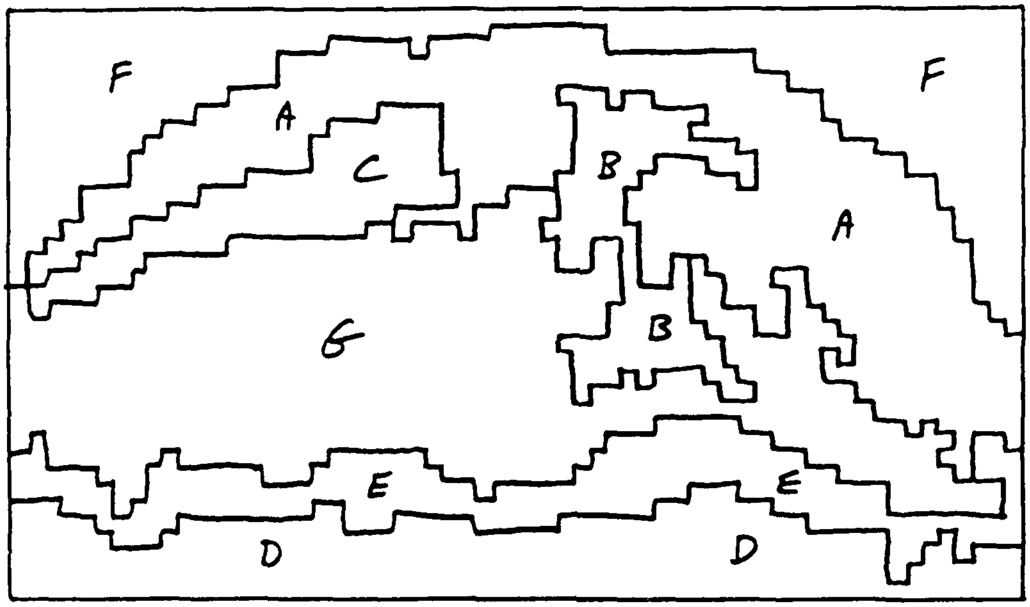

Figure 5b. As in Fig. 2b except for HSWO segmentation using cost function in Eqn. (2).

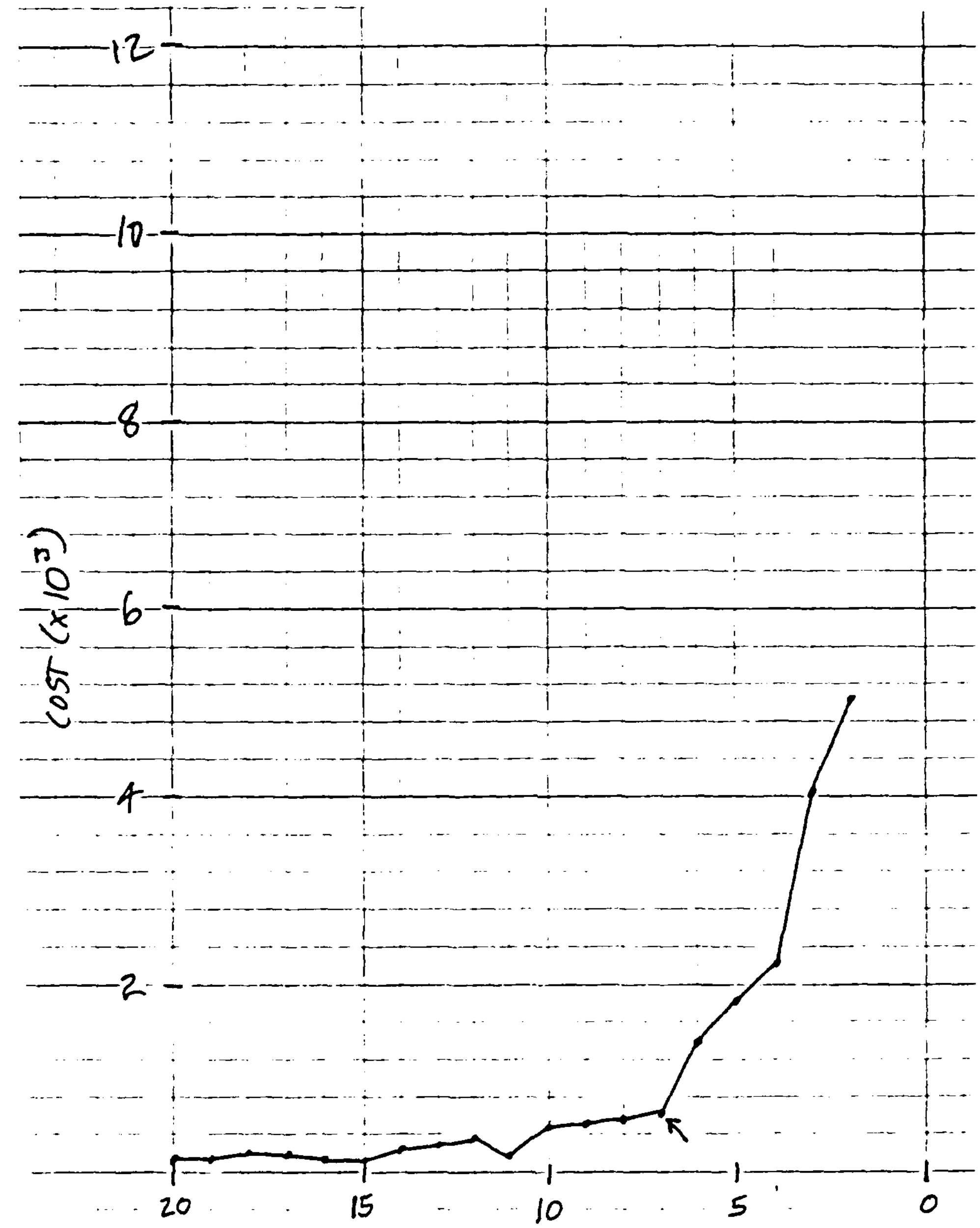

Figure 5c. As in Fig. 2c except for HSWO segmentation using cost function in Eqn. (2).

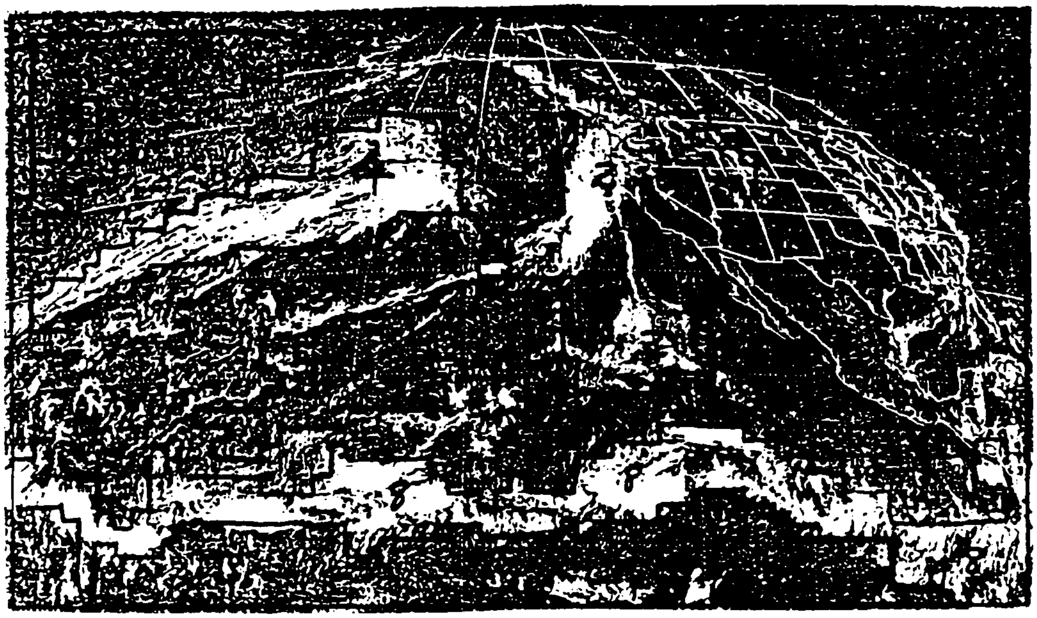

Figure 6a. As in Fig. 2a except for HSWO segmentation using cost function in Eqn. (3).

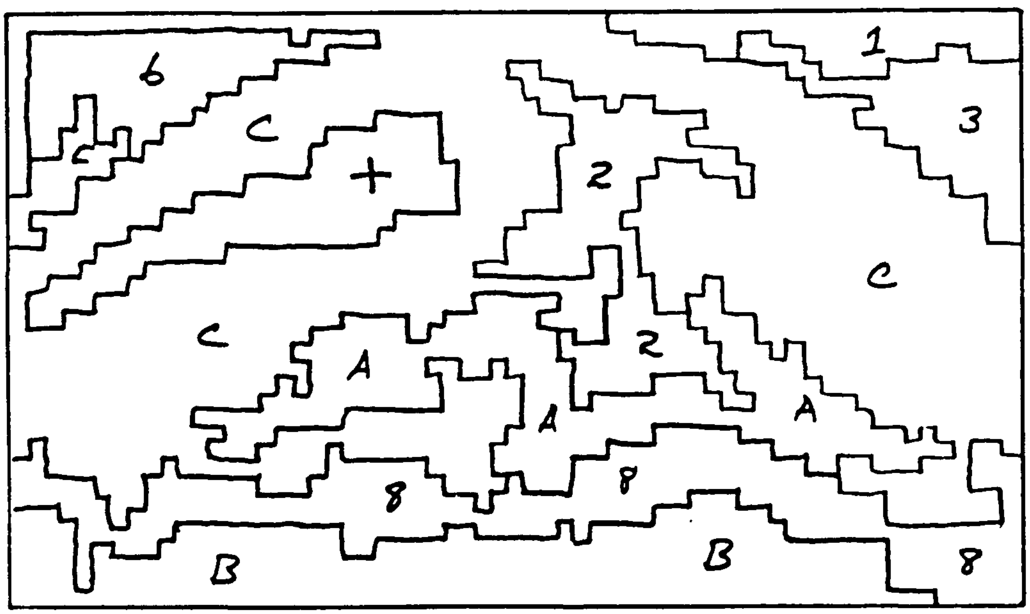

Figure 6b. As in Fig. 2b except for HSWO segmentation using cost function in Eqn. (3).

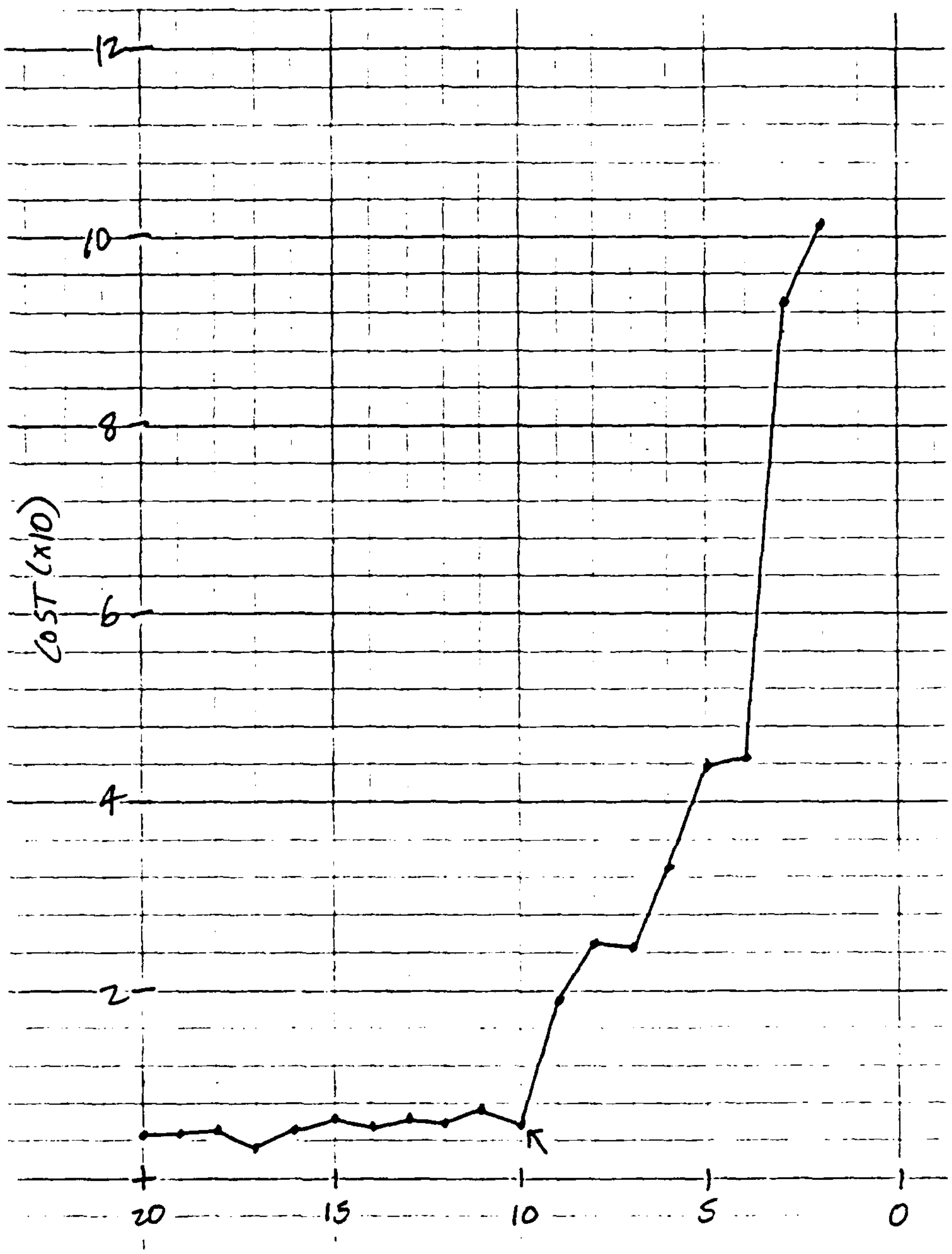

Figure 6c. As in Fig. 2c except for HSWO segmentation using cost function in Eqn. (3).

the cost of combining dark regions is now so high that these false details occur. The stratocumulus region is still included in the eastern front (area 2), but notice that more of the thin, tailing portion is now included as well. Thus, the new cost function is beginning to have the desired effect. It may seem that the anomalous detail in the dark regions would be a problem. However, we are only interested in segmenting the cloudy areas well so that they can be classified later. Thus, in the actual use of these segmentations one could simply refer to the average grayshade of each region and discard those that are too dark to be cloud features.

The segmentation still fails to incorporate the entire eastern front. We can increase the effect of the grayshade term in the denominator by omitting its nonlinear portion. In other words, rather than squaring the sum of the two grayshades, simply square each individual grayshade:

$$C_{i,j} = \frac{N_i * N_j}{N_i + N_j} * \frac{(x_i - x_j)^2}{x_i^2 + x_j^2} \qquad (4)$$

This final segmentation is presented in Fig. 7. The western front (A) now includes some of the broken cloudiness scuth of its tail, but the overall shape is still correct. The ITCZ (area ¯) still spans the image nicely. The broken cloudiness north of the ITCZ is assigned its own region (area 9) and the outer space regions continue to have anomalous detail (areas 1, 3, ^ and +). The most encouraging aspect of this segmentation is its ability to include the entire eastern front (area C). The region continues to include the stratocumulus area as well. This error seems

Figure 7a. As in Fig. 2a except for HSWO segmentation using cost function in Eqn. (4).

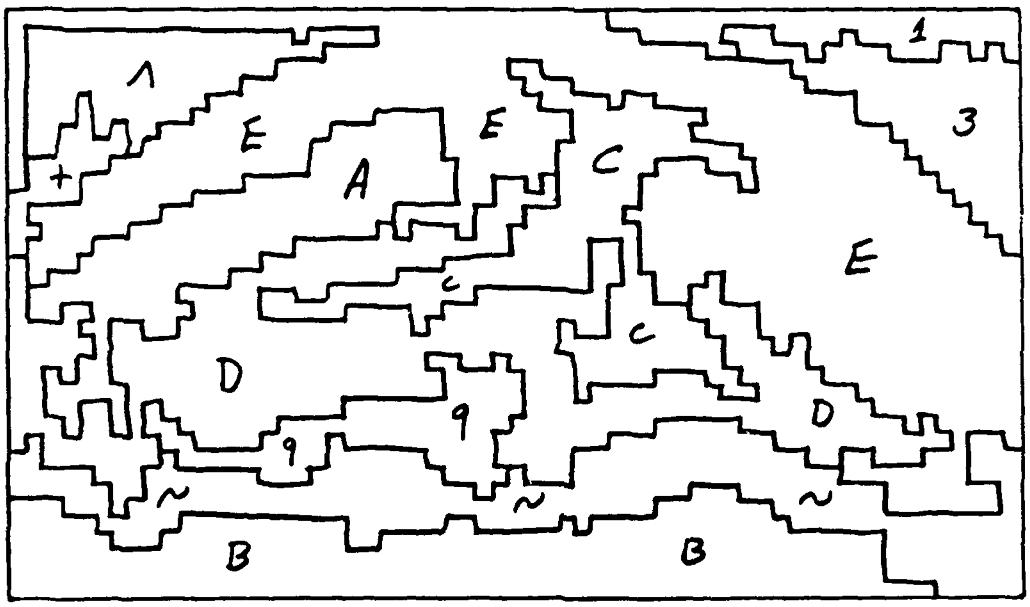

Figure 7b. As in Fig. 2b except for HSWO segmentation using cost function in Eqn. (4).

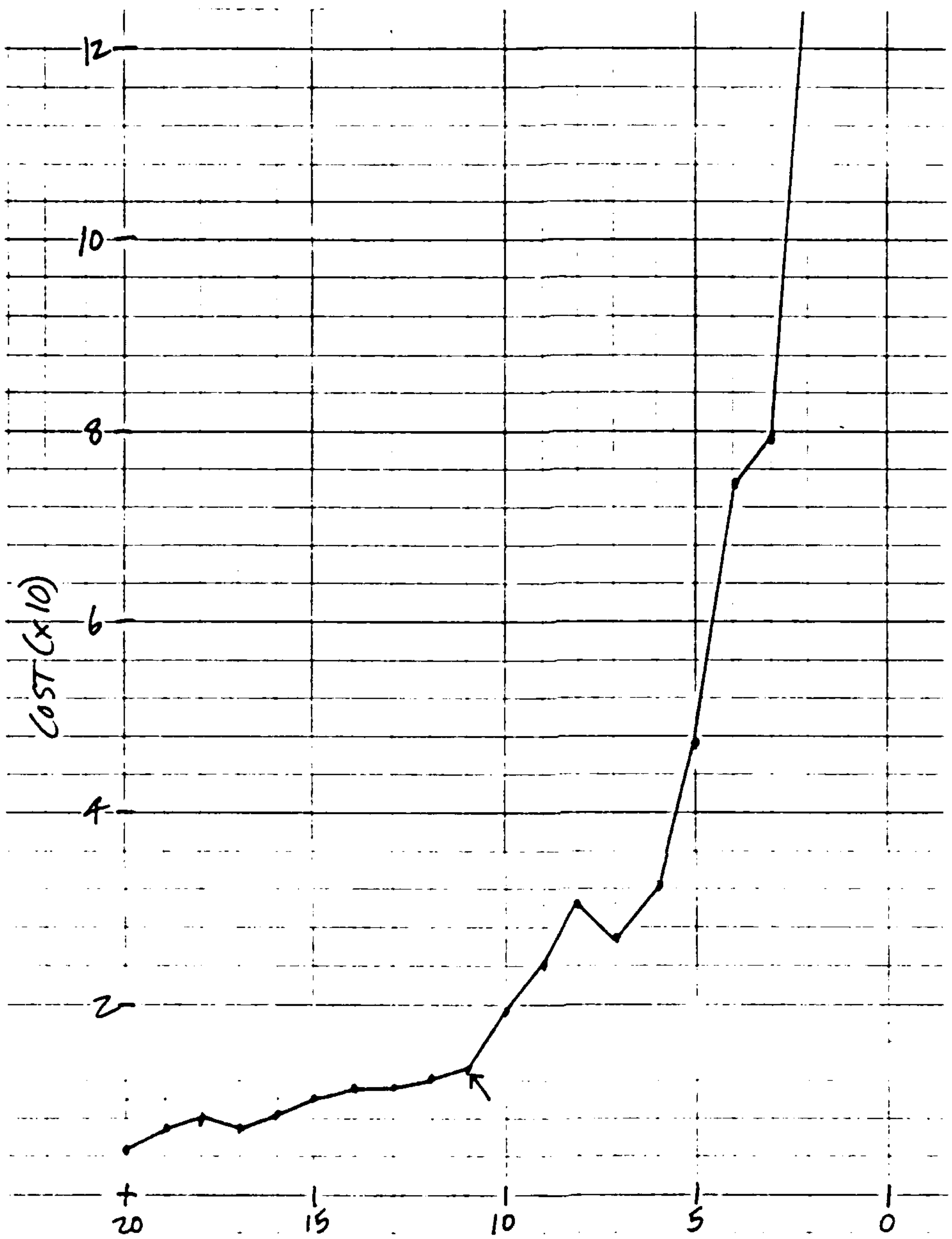

Figure 7c. As in Fig. 2c except for HSWO segmentation using cost function in Eqn. (4).

unavoidable because the connecting cloud band is so bright. It would be difficult to come up with a scheme that separates these two regions while also connecting the eastern front with its tail.

There are likely many such problem cases that arise in such cloud scenes. To come up with a meaningful segmentation would seem to require some top-level information to resolve such problem areas. Regions, such as the western front, that fit the classical model of such features and are not connected or adjacent to other cloudy areas can be easily segmented. However, problem regions such as area C (Fig. 7) would require some post-processing to determine that the stratocumulus area should be separated from the frontal band.

Finally, the stopping criterion should be examined in these cases. Figures 2c - 7c reveal that the cloud imagery exhibits a similar minimum cost function jump as that demonstrated by Beulieu and Goldberg (1989). The choice of stopping point based on these curves is fairly straightforward. A closer examination of the errors in the various segmentations reveals that the particular choice of stopping point is usually not the cause of the errors. Combinations that should not have occurred typically happen several iterations prior to the selected stopping point. Similarly, combinations that should have occurred would not have happened until many iterations after the stopping points. There fore, the important issue seems to be the HSWO scheme itself (e.g., the choice of cost function) rather than the stopping point.

4. Case Studies

In this section six case studies of the HSWO routine will be presented. The images chosen are taken every three days from Oct. 1 - Oct. 16, 1983. As a basis for comparison, the original HSWO segmentations are presented along with the segmentations that result from the use of the new cost function in Eqn. (4). As will be shown, these cases contain very complex cloud regions rather than the nice, isolated features such as those seen in the Nov. 15 case.

4.1 October 1, 1983 Case

This case is characterized by a large, frontal band extending from the Bering Sea to the southwest edge of the image (Fig. 8). There is a cloud vortex west of Hawaii that indicates a cutoff low. The area from Hawaii to the U.S. west coast is characterized by stratocumulus cells. A frontal band extends from the Rockies southwest to the ocean west of Baja. The ITCZ spans the tropics and includes a tropical cyclone in the east Pacific.

The segmentation using the original HSWO scheme is presented in Fig. 9. The western front has been divided into two, adjacent regions (areas 6 & 12). The cloud vortex has been well-defined in region 9. The stratocumulus area is absorbed into background areas 2 and 3. The eastern front (area 5) is handled well. There is a lot of fine detail included in the ITCZ (areas 4, 8, 10, 11, 15, 19 and 22) although such detail brings out the tropical cyclone (area 7). The stopping criterion for this case (Fig. 9c) is based on a relatively small jump at 15 regions. If the

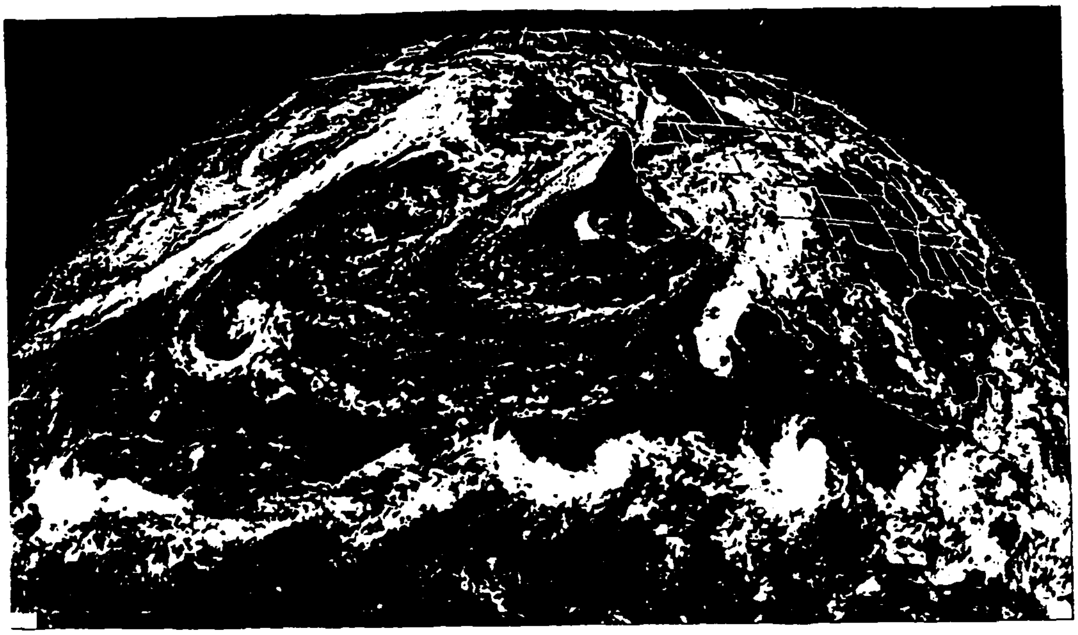

Figure 8. As in Fig. 1 except for Oct. 1, 1983 image.

Figure 9a. As in Fig. 2a except for original HSWO segmentation using image in Fig. 8.

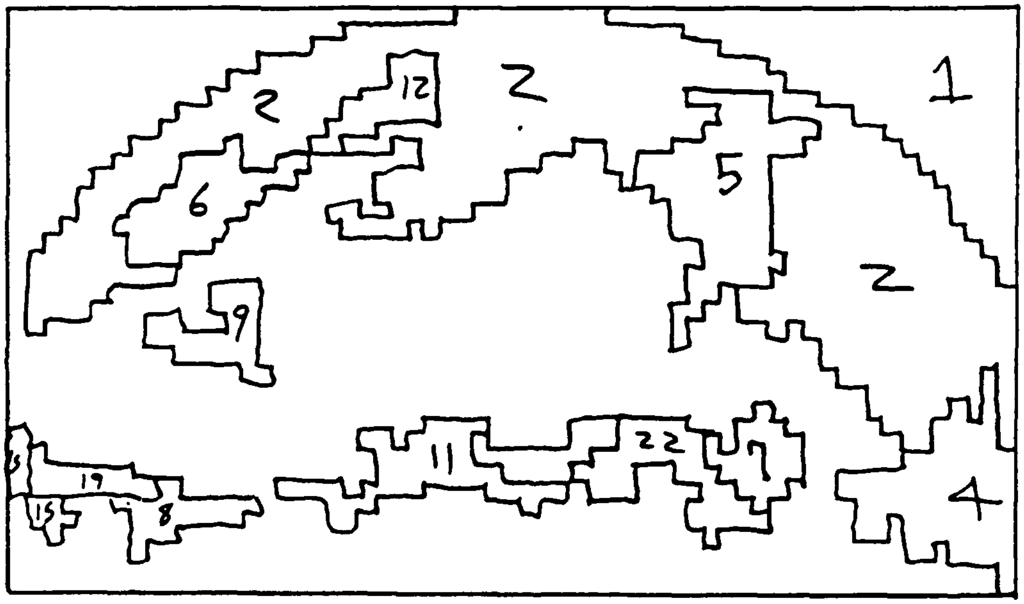

Figure 9b. As in Fig. 2b except for original HSWO segmentation using image in Fig. 8.

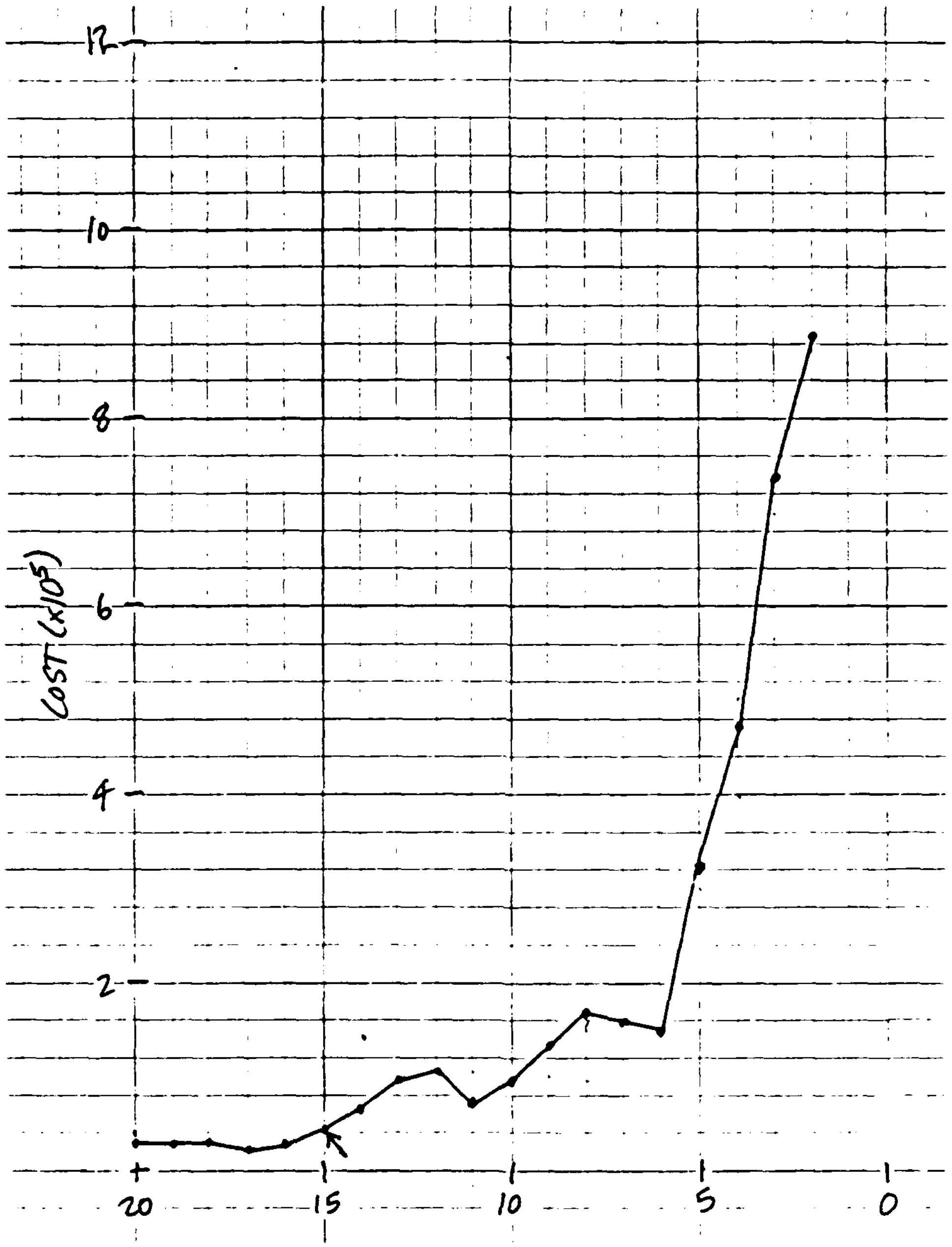

Figure 9c. As in Fig. 2c except for original HSWO segmentation using image in Fig. 8.

jump at 11 regions had been used, much of the ITCZ detail would have been combined.

When using the new segmentation based on Eqn. (4), the image again contains much more detail (Fig. 10). The western front (area 8) is now one complete region. It is curious that the southmost portion of the front is still separated, and is, in fact, combined with the clouds associated with the cutoff low. For this feature, the original HSWO appears superior. Neither scheme handles the stratocumulus region well. The eastern front is well-handled by both schemes. One advantage in the new scheme is that the ITCZ is resolved as one, large band. The tropical cyclone, however, is not resolved by this method. As stated in the previous section, the anomalous detail in the dark regions can be easily handled in post-processing.

Neither scheme is the clear winner on this case. It is important that the western front be resolved as one band, but the failure to isolate the cutoff low by the new scheme is disappointing.

4.2 Oct. 4, 1983 Case

This case (Fig. 11) has a very complex cloud region in the Bering Sea. R. Fett identified a nearly east-west oriented frontal band with open cells to the north and stratocumulus to the south. He also identified the bright clouds at the tip of the Alleutians as another frontal band. The bright area west of California is dense fog. The same frontal band seen on the Oct. 1 image over Baja is seen here (this may not be a front after all), along with the tropical cyclone now to the north of the

Figure 10a. As in Fig. 2a except for HSWO segmentation on image in Fig. 8 using cost function in Eqn. (4).

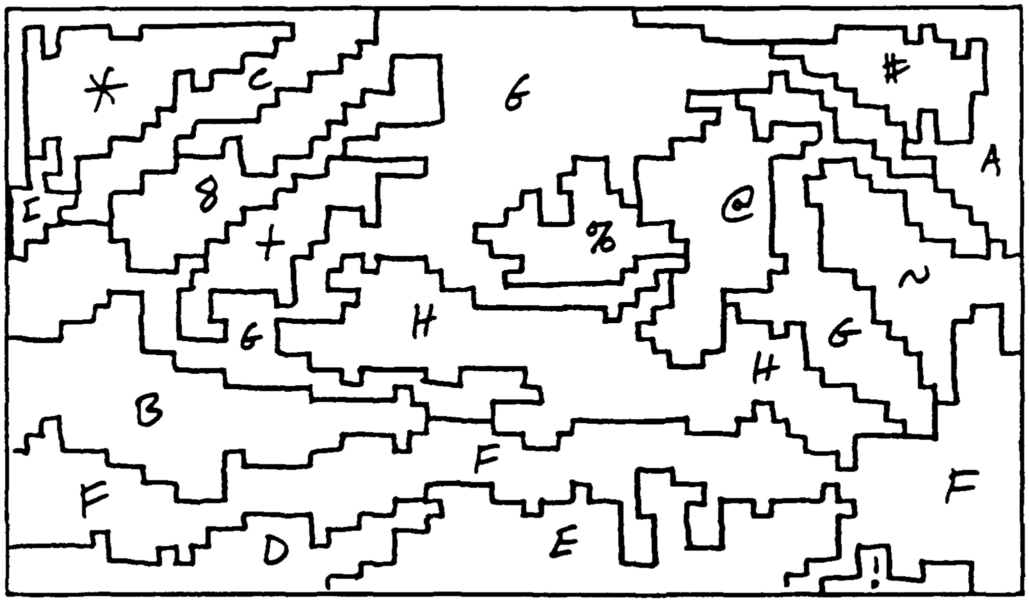

Figure 10b. As in Fig. 2b except for HSWO segmentation on image in Fig. 8 using cost function in Eqn. (4).

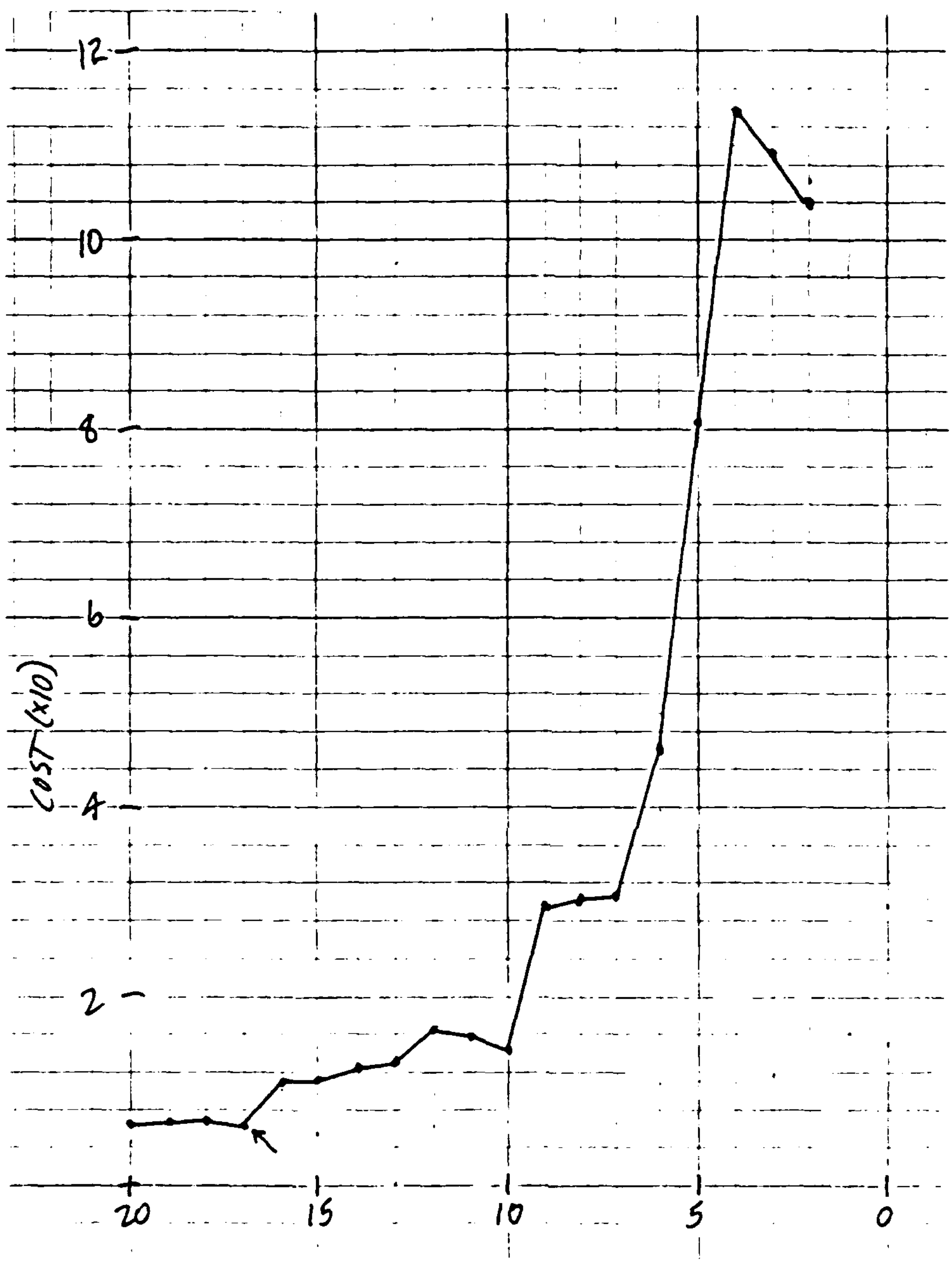

Figure 10c. As in Fig. 2c except for HSWO segmentation on image in Fig. 8 using cost function in Eqn. (4).

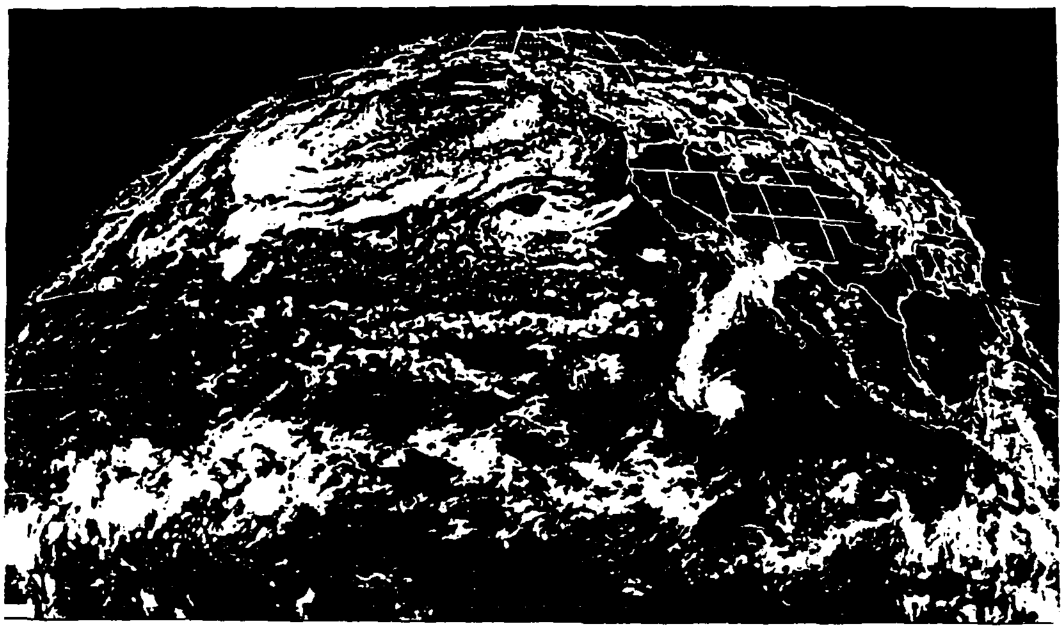

Figure 11. As in Fig. 1 except for Oct. 4, 1983 image.

ITCZ. The ITCZ is most active in the west, with a clear break south of the tropical cyclone.

The HSWO (Fig. 12) isolates the Bering cold fronts into a single region (area 7). This region also includes some of the open cells to the north and the fog region. The stratocumulus region is absorbed into background area 4. The Baja cloud band is well-defined (area 5). There is much structure in the ITCZ here as well.

The modified HSWO (Fig. 13) handles the complex Bering fronts in a similar fashion. The Baja front (area ^) is also well-handled. There is not quite as much complexity in the ITCZ, although the central portion has been combined into the background area A.

Again, there is no clear superiority of either scheme. This image contains some very complex features that are difficult for even an expert to segment correctly without using some top-level knowledge of what the features might be.

4.3 Oct. 7, 1983 Case

The cloud band in the extreme west (Fig. 14) is a meridional trough. There is a front in the Bering Sea with a vortex to the south and a thin, dissipating front extending toward Hawaii. There is dense fog off the northern California coast and the remnants of the tropical cyclone over southern California.

The segmentation (Fig. 15) again handles the complex Bering sea features by combining them into a single region B. The dissipating front is completely lost. The meridional trough appears as two, separate regions D and F. The tropical cyclone

Figure 12a. As in Fig. 2a except for original HSWO segmentation using image in Fig. 11.

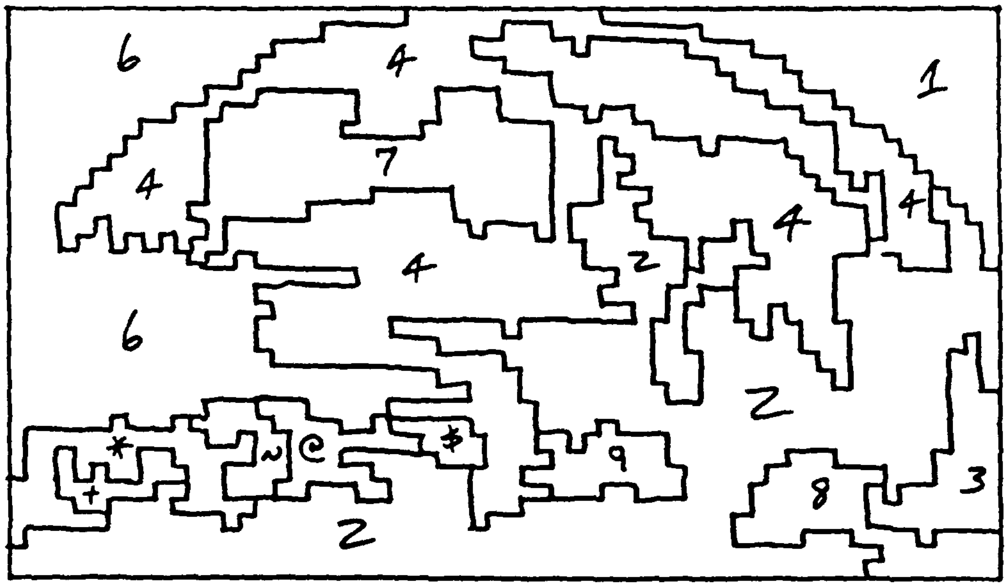

Figure 12b. As in Fig. 2b except for original HSWO segmentation using image in Fig. 11.

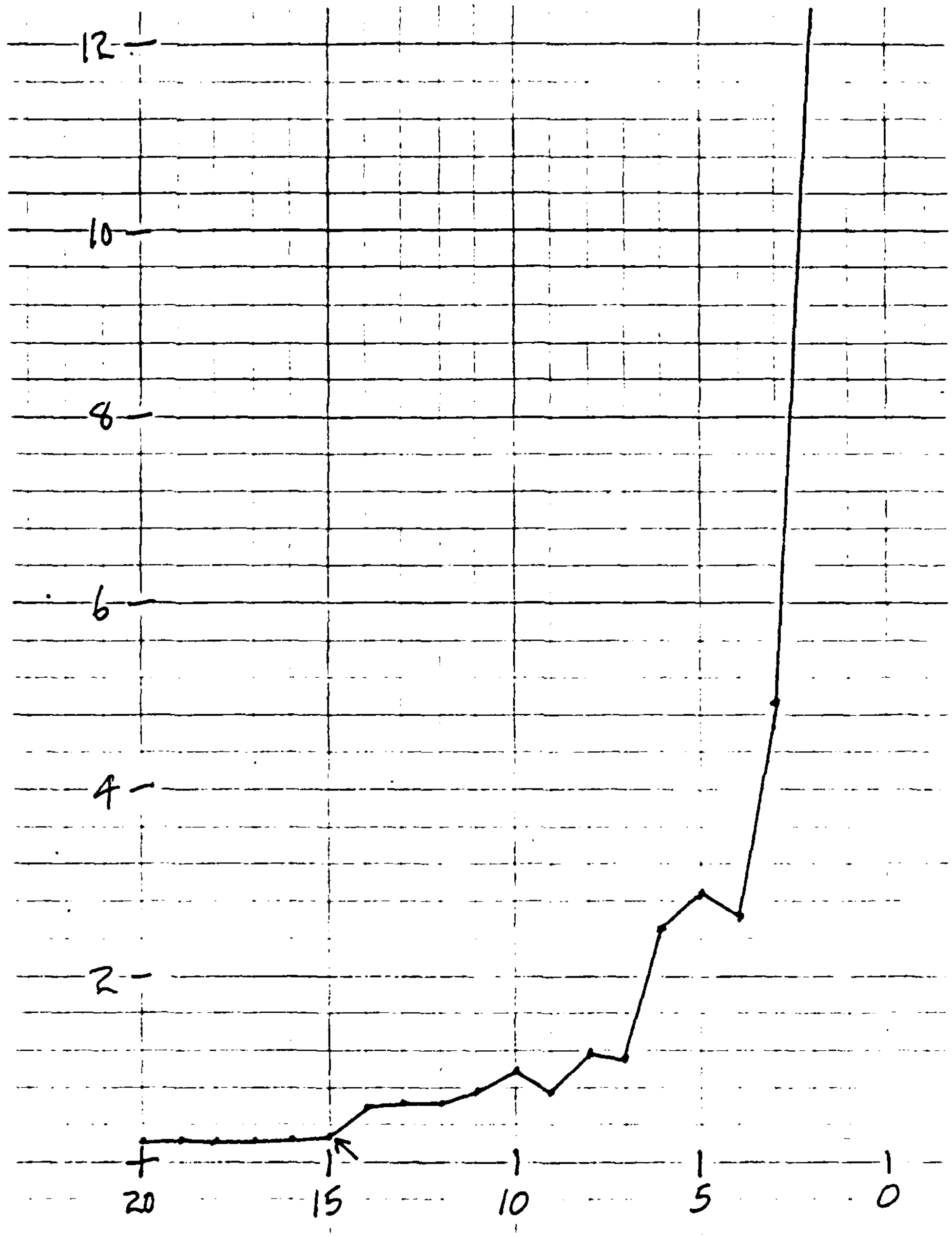

Figure 12c. As in Fig. 2c except for original HSWO segmentation using image in Fig. 11.

Figure 13a. As in Fig. 2a except for HSWO segmentation on image in Fig. 11 using cost function in Eqn. (4).

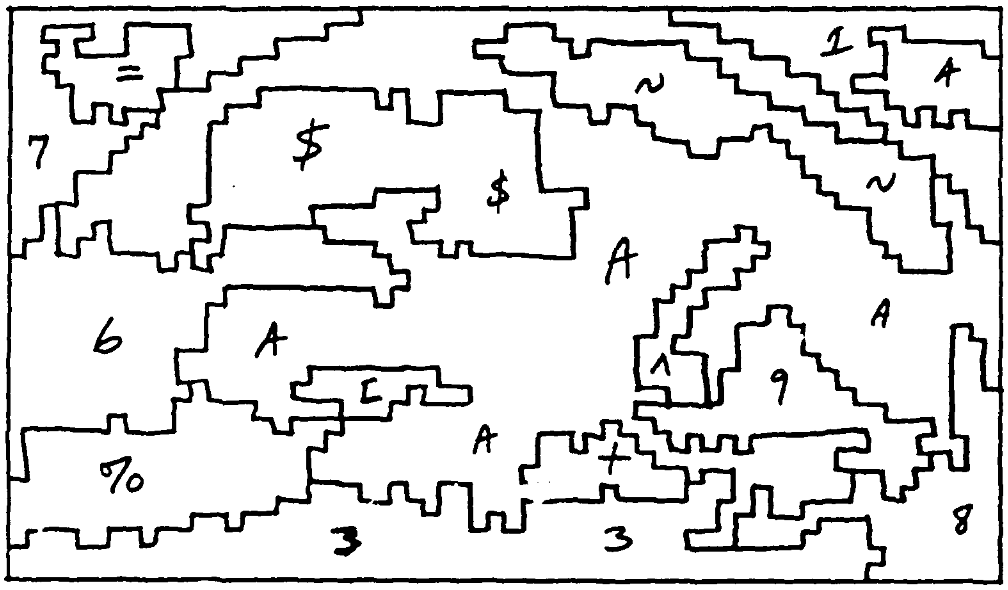

Figure 13b. As in Fig. 2b except for HSWO segmentation on image in Fig. 11 using cost function in Eqn. (4).

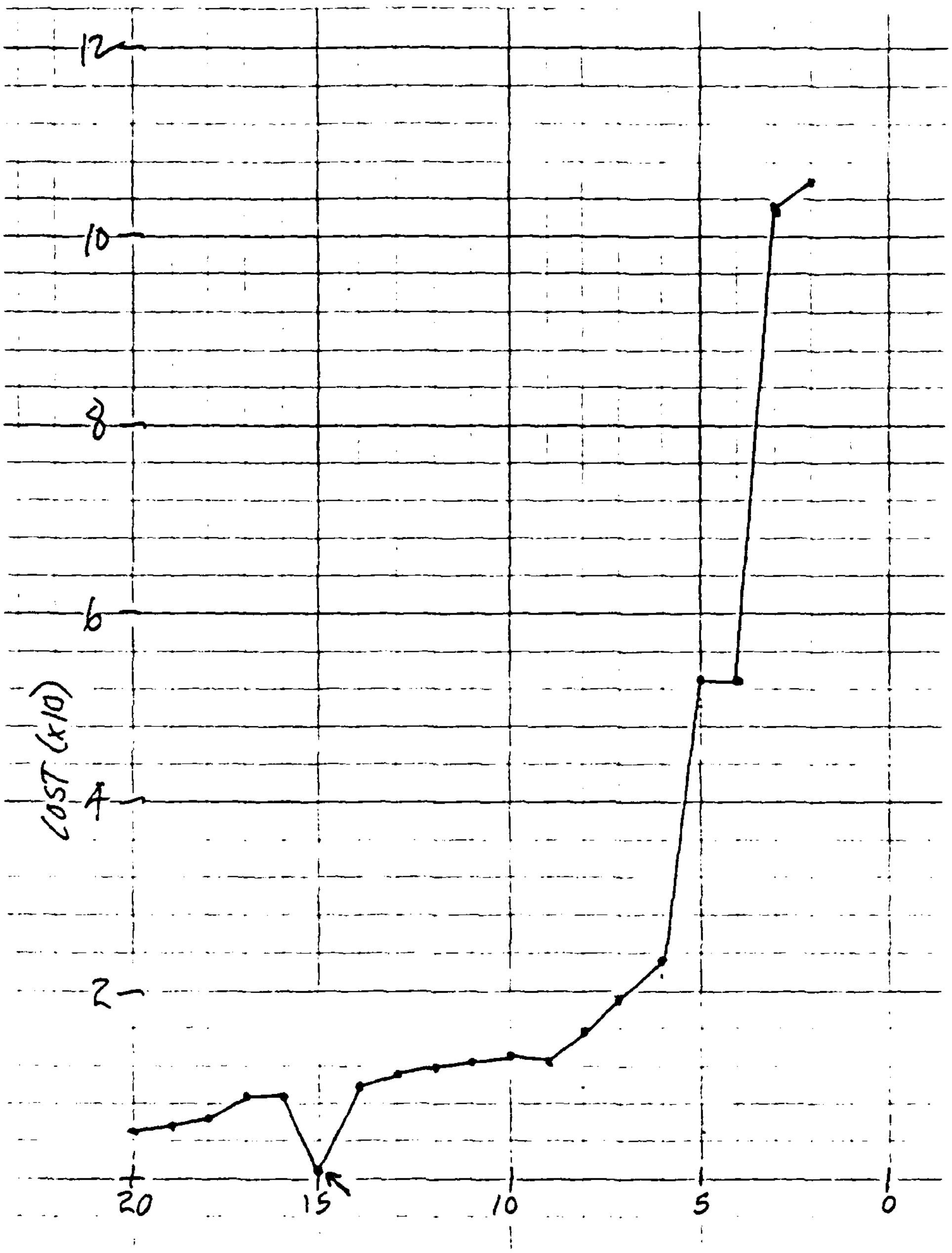

Figure 13c. As in Fig. 2c except for HSWO segmentation on image in Fig. 11 using cost function in Eqn. (4).

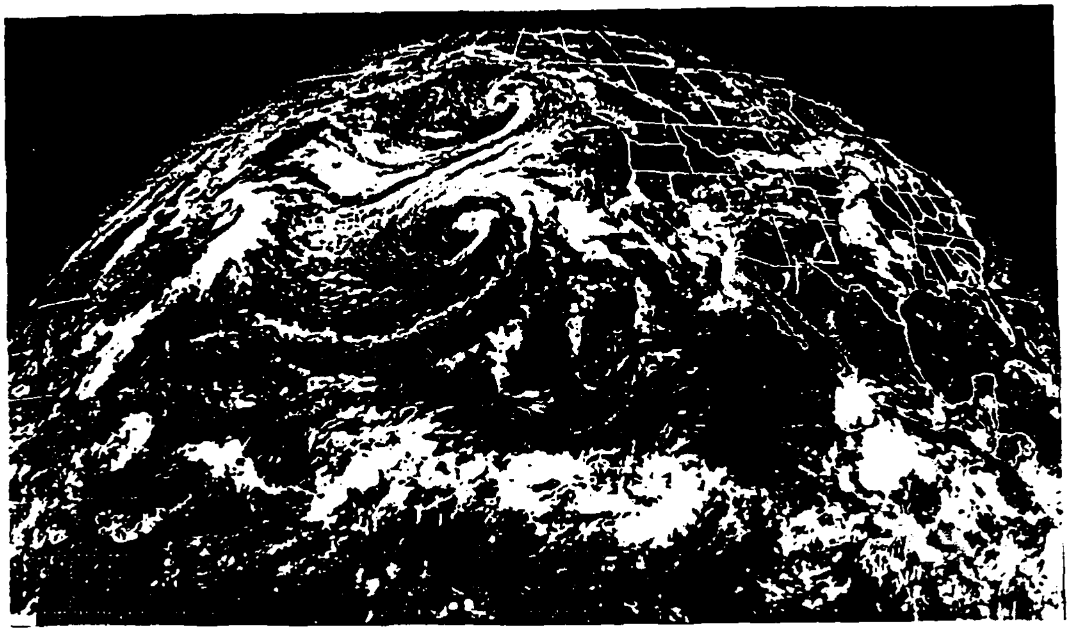

Figure 14. As in Fig. 1 except for Oct. 7, 1983 image.

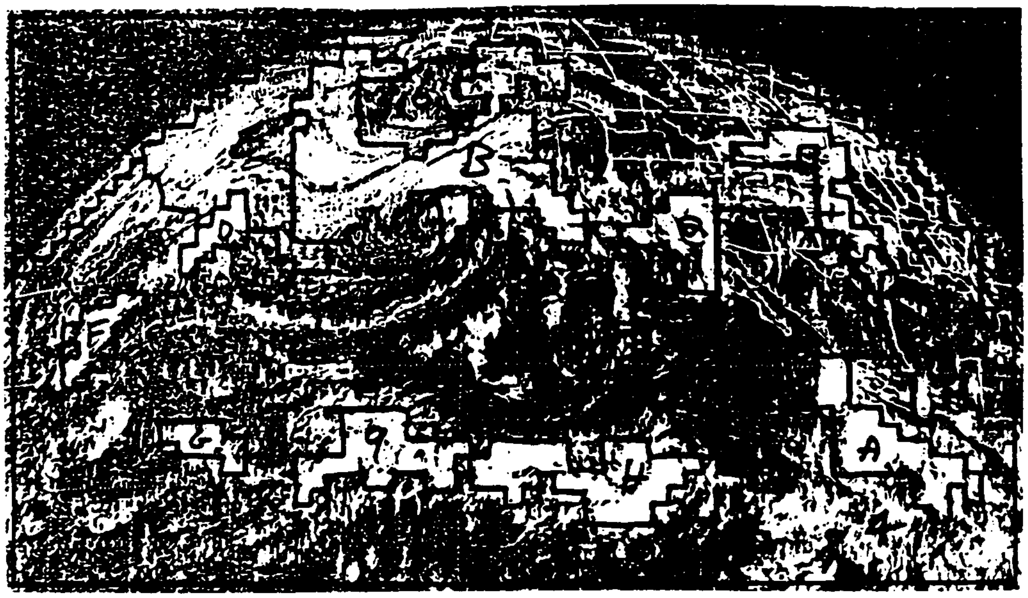

Figure 15a. As in Fig. 2a except for original HSWO segmentation using image in Fig. 14.

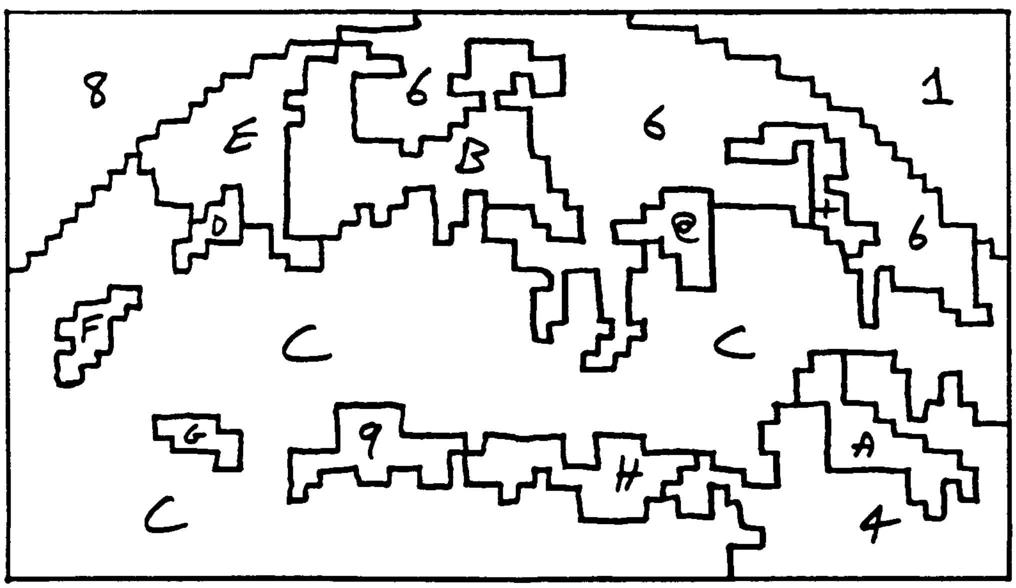

Figure 15b. As in Fig. 2b except for original HSWO segmentation using image in Fig. 14.

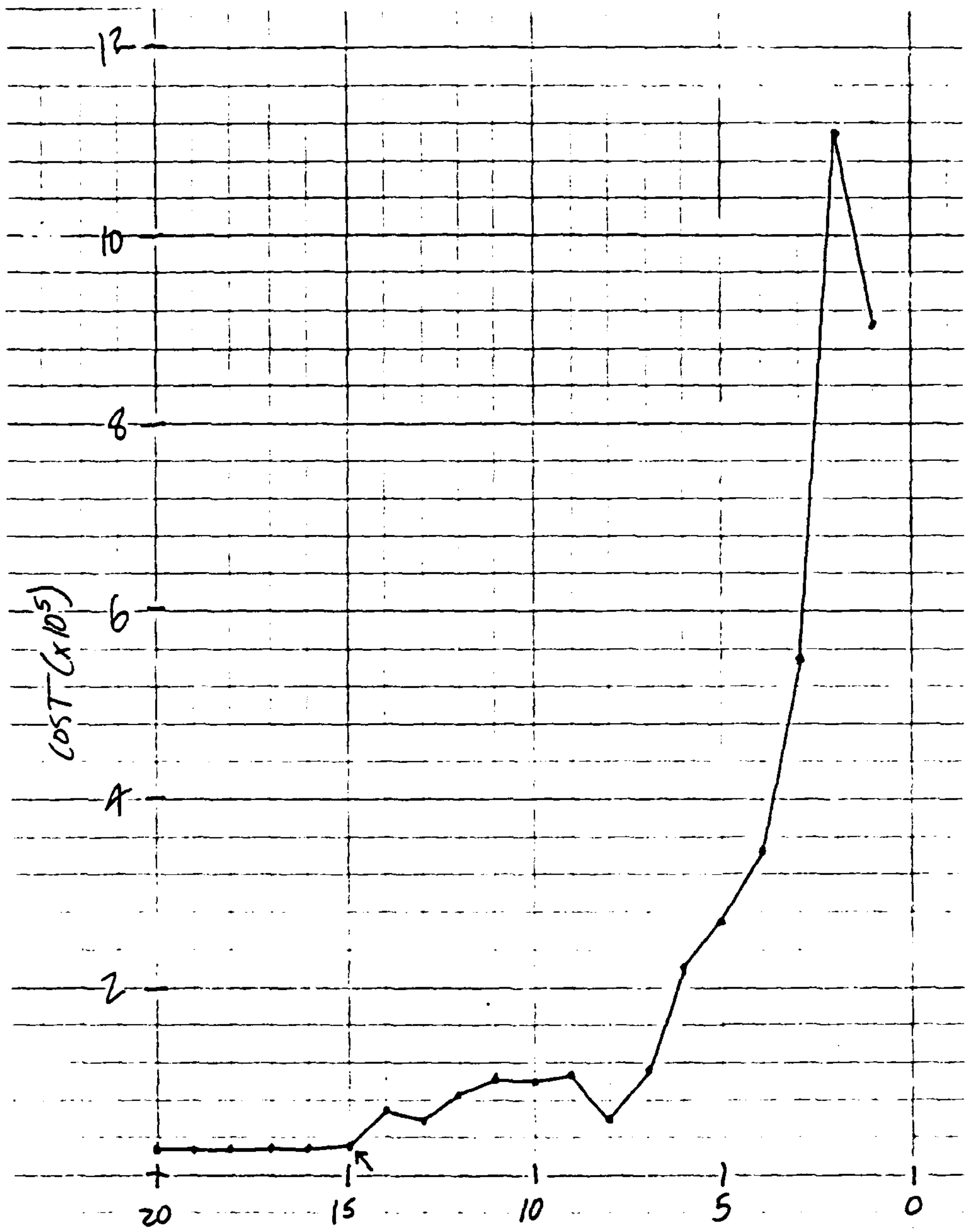

Figure 15c. As in Fig. 2c except for original HSWO segmentation using image in Fig. 14.

is handled well (area @) and there is the typical overstructuring of the ITCZ (areas 4, 9, A and G).

The modified HSWO segmentation (Fig. 16) also has difficulty with the Bering Sea features, but makes matters even worse by extending the region (area @) across the western U.S. The meridional trough is combined with the dim clouds to the west (area ~). Even the tropical cyclone is not resolved here. The one good point is that the ITCZ is resolved as a single, continuous band.

The original segmentation seems to be better here if one is interested in resolving the mid-latitude features, although considerable post-processing would still be required. The modified HSWO seems to handle the ITCZ better, in general.

4.4 Oct. 10, 1983 Case.

This case (Fig. 17) finally departs from the very complex features to a more "normal" scene. There is a frontal band extending from Alaska to the southwest. Ahead of the front is a vortex associated with an upper cold low. West of Baja is a stratocumulus region and a hurricane to the south.

Unlike the other cases, the cost function curve of this case (Fig. 18c) had no good stopping point short of only six regions. In that case (not shown), only the frontal band is resolved, and the remaining areas are background regions. If we accept a 35% rise in cost as a cutoff, one can stop at 19 regions (Fig. 18c). This situation is shown in Fig. 18a & b. Here the front is resolved well (area 5). The vortex is partially resolved, but it is also included into the cloudy region over the northwest U.S.

Figure 16a. As in Fig. 2a except for HSWO segmentation on image in Fig. 14 using cost function in Eqn. (4).

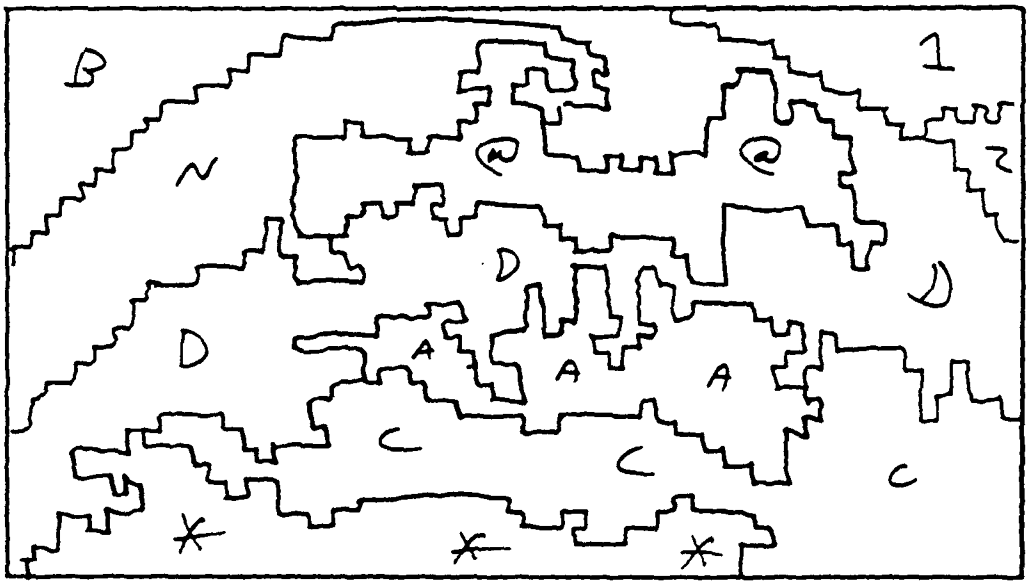

Figure 16b. As in Fig. 2b except for HSWO segmentation on image in Fig. 14 using cost function in Eqn. (4).

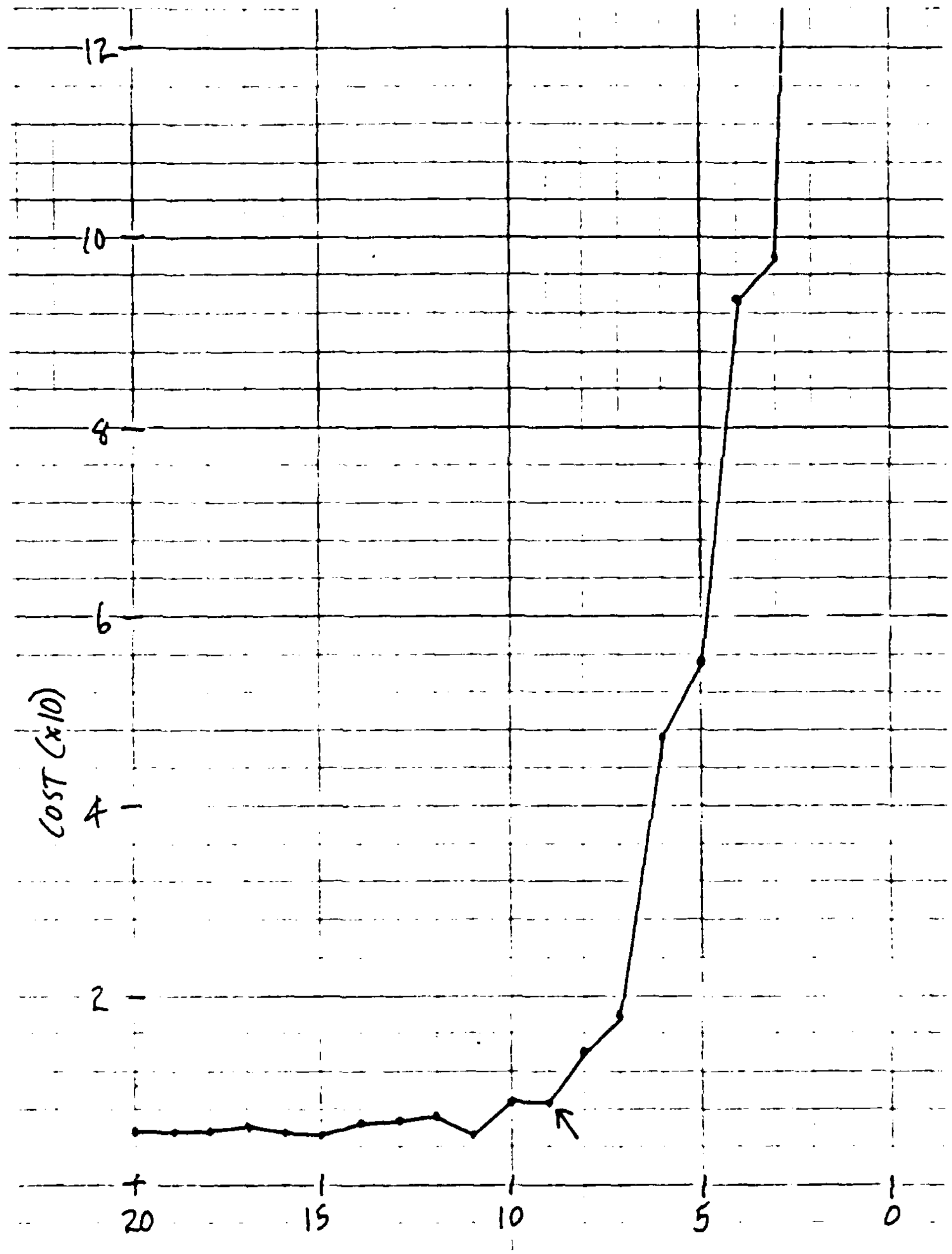

Figure 16c. As in Fig. 2c except for HSWO segmentation on image in Fig. 14 using cost function in Eqn. (4).

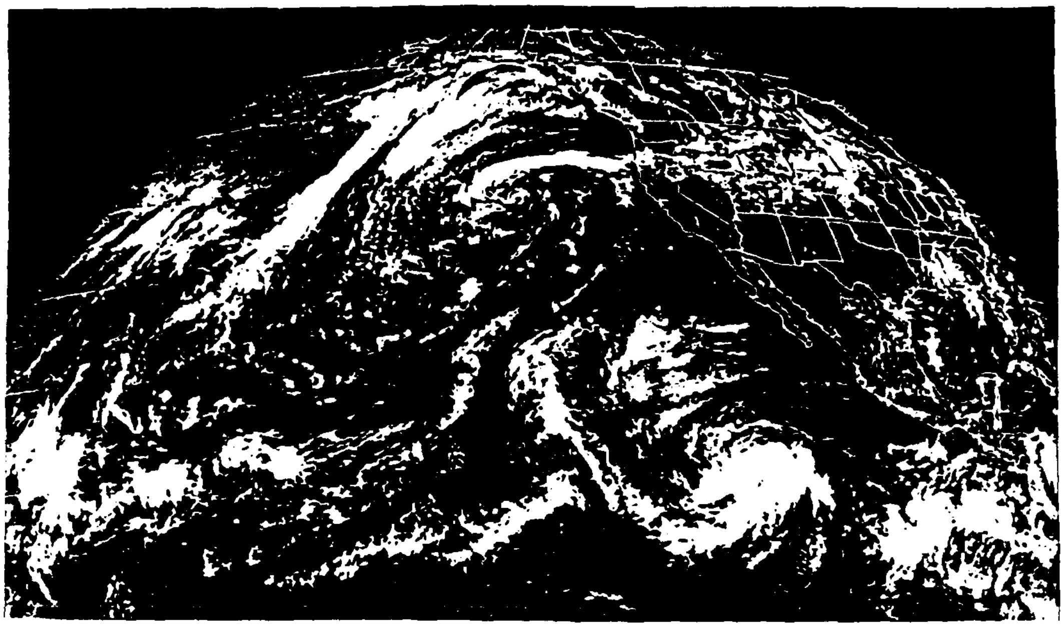

Figure 17. As in Fig. 1 except for Oct. 10, 1983 image.

Figure 18a. As in Fig. 2a except for original HSWO segmentation using image in Fig. 17.

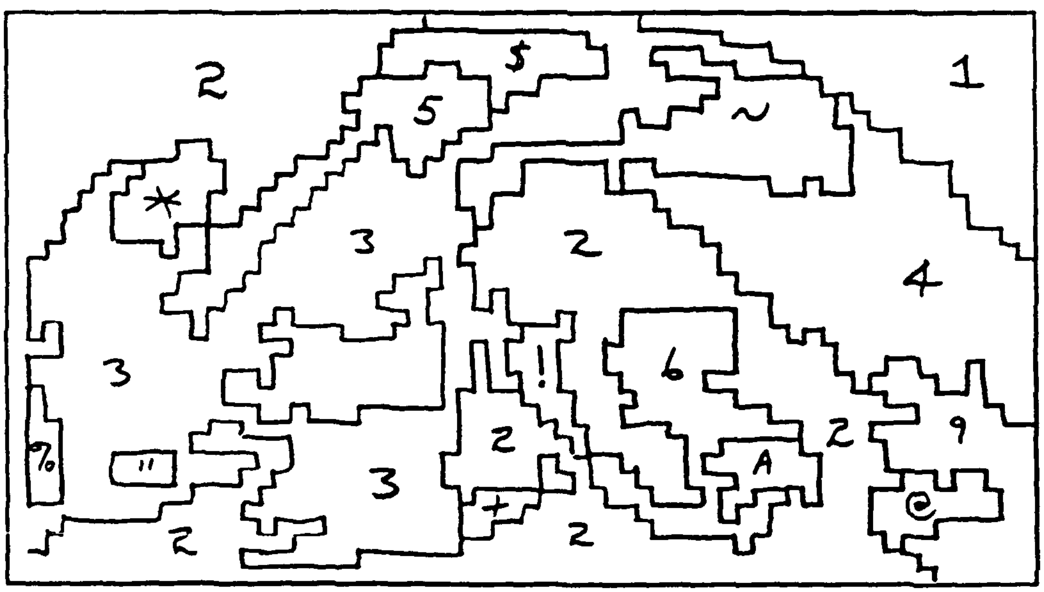

Figure 18b. As in Fig. 2b except for original HSWO segmentation using image in Fig. 17.

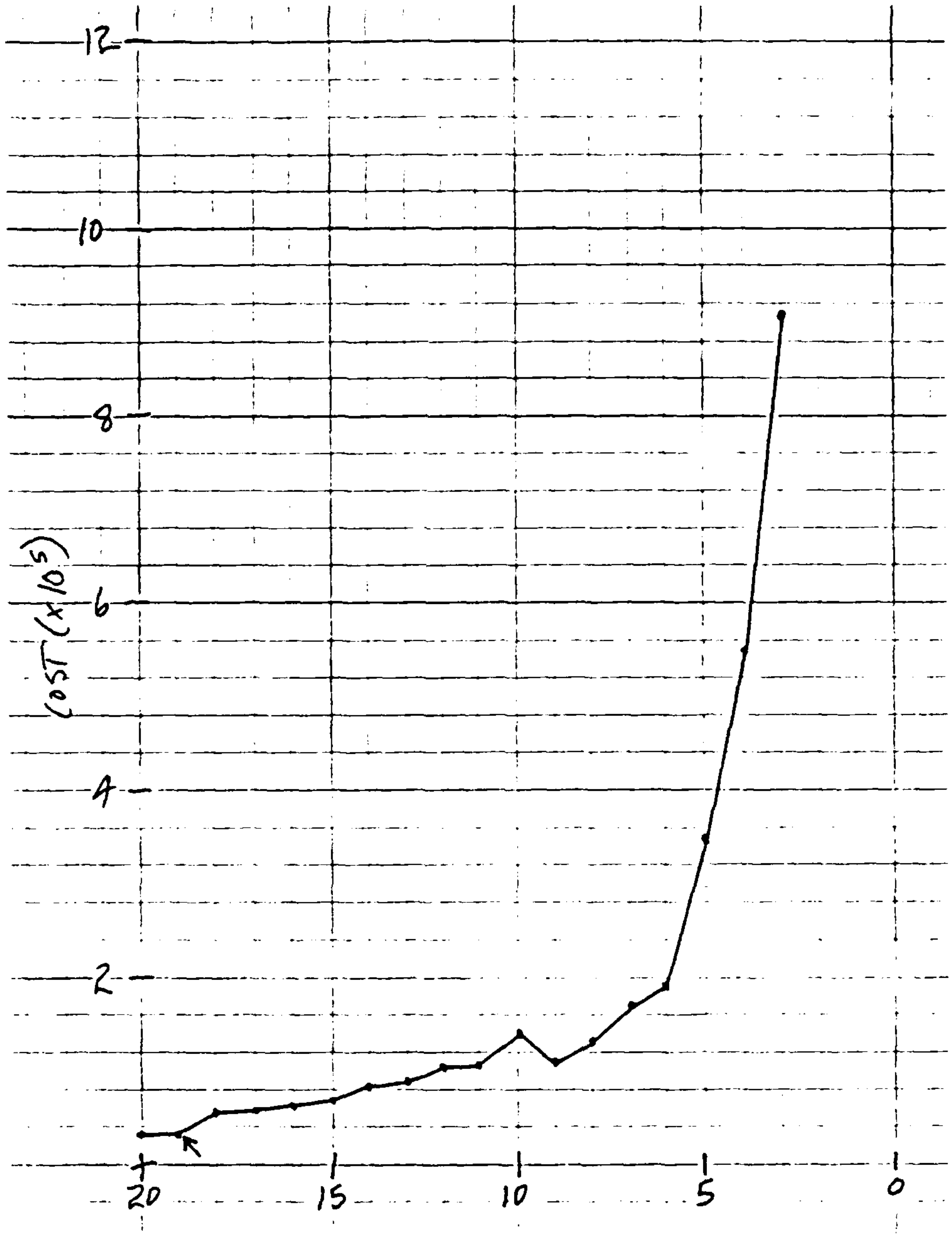

Figure 18c. As in Fig. 2c except for original HSWO segmentation using image in Fig. 17.

(area ~). The stratocumulus region is resolved (area 6) as is the hurricane (area A). Again, there is much structure assigned to the ITCZ and background regions.

The modified HSWO (fig. 19) also resolves the front well (area -) and the vortex is again included into the cloudy region to the east (area <). Here, the hurricane and stratocumulus regions are combined (area D) along with a portion of the ITCZ. The original HSWO is clearly superior in this case.

4.5 Oct. 13, 1983 Case.

In this image (Fig. 20) there is a broad, frontal band extending from the Alleutians to the southwest. There is another, thin front to the east in the Bering Sea. There is an area of stratocumulus off the northern California coast and another one northwest of a large hurricane.

The segmentation of this image (Fig. 21) captures the large front well (area B), but the northern stratocumulus area is also incorporated. The hurricane (area C) is well handled, but the southern stratocumulus area is combined into background area A. Major features of the ITCZ are isolated (areas 3, 7, 8, + and !).

The modified HSWO (Fig. 22) also does well in isolating the broad front (area *), and this method does not incorporate the northern stratocumulus area. Unfortunately, that area is absorbed into background region 5. The hurricane is segmented into area <. Here, the southern stratocumulus area gets absorbed into the western ITCZ. The scheme is, however, able to isolate the southern portion of the thin front (area +), although some of the western portion of this region is background.

Figure 19a. As in Fig. 2a except for HSWO segmentation on image in Fig. 17 using cost function in Eqn. (4).

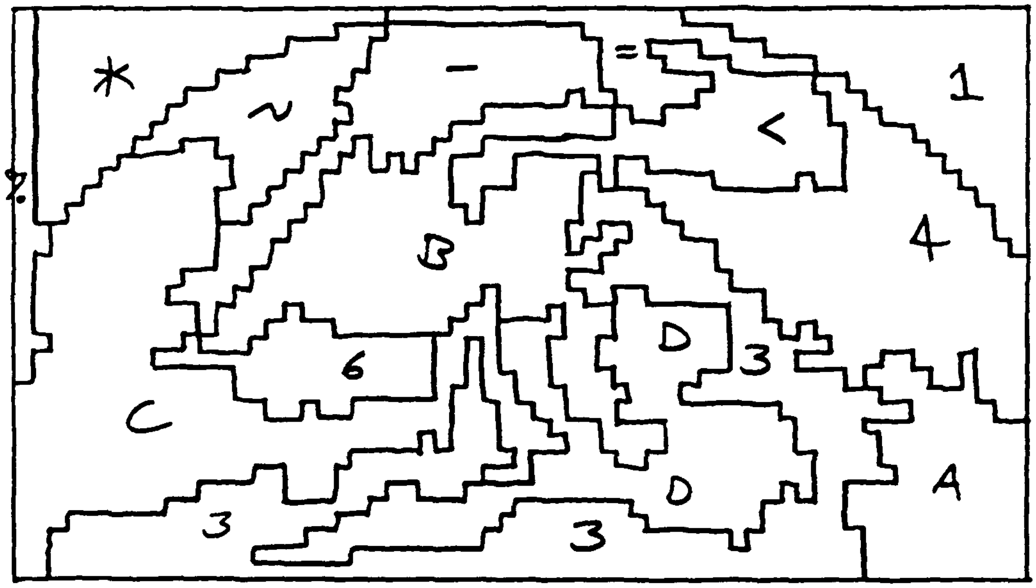

Figure 19b. As in Fig. 2b except for HSWO segmentation on image in Fig. 17 using cost function in Eqn. (4).

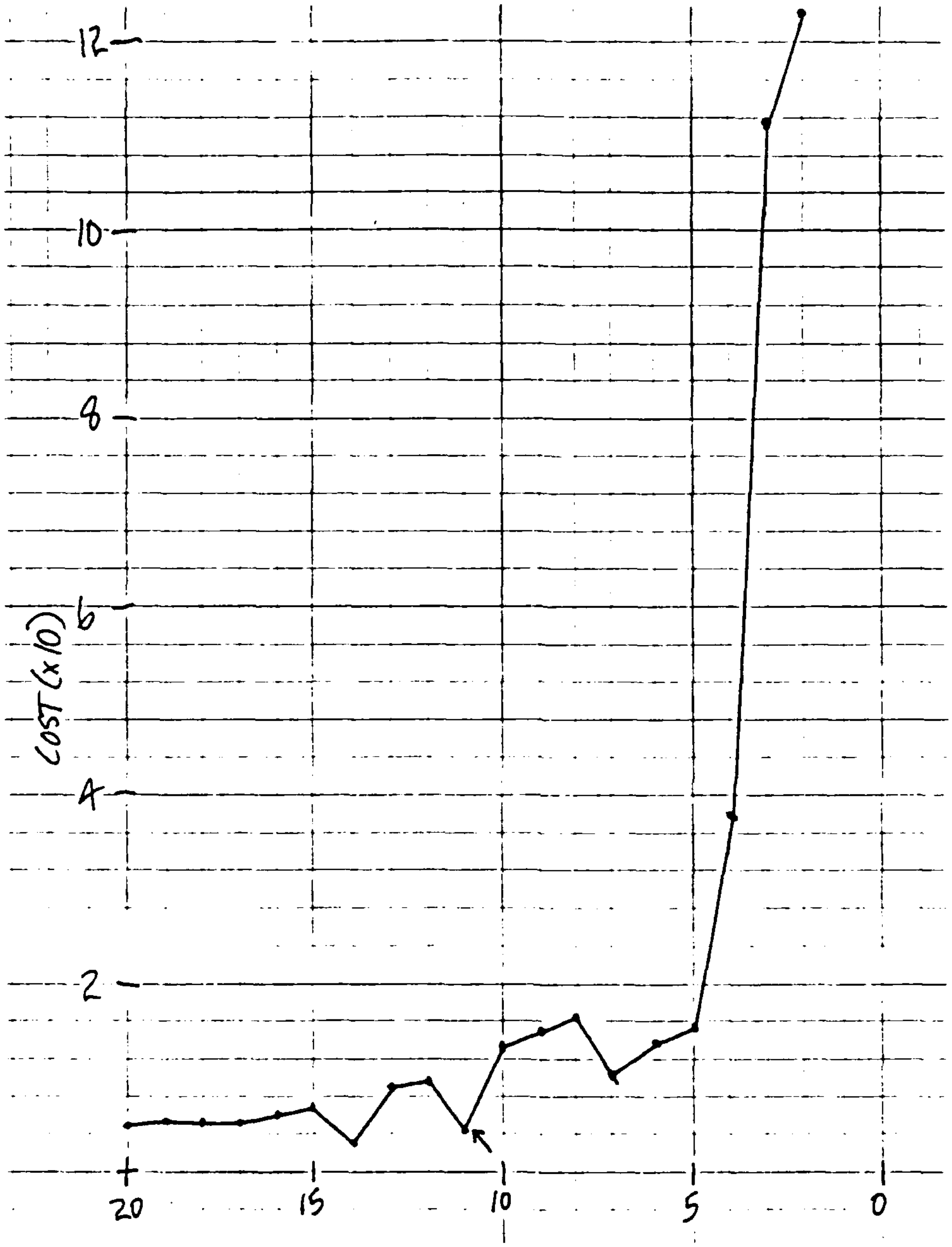

Figure 19c. As in Fig. 2c except for HSWO segmentation on image in Fig. 17 using cost function in Eqn. (4).

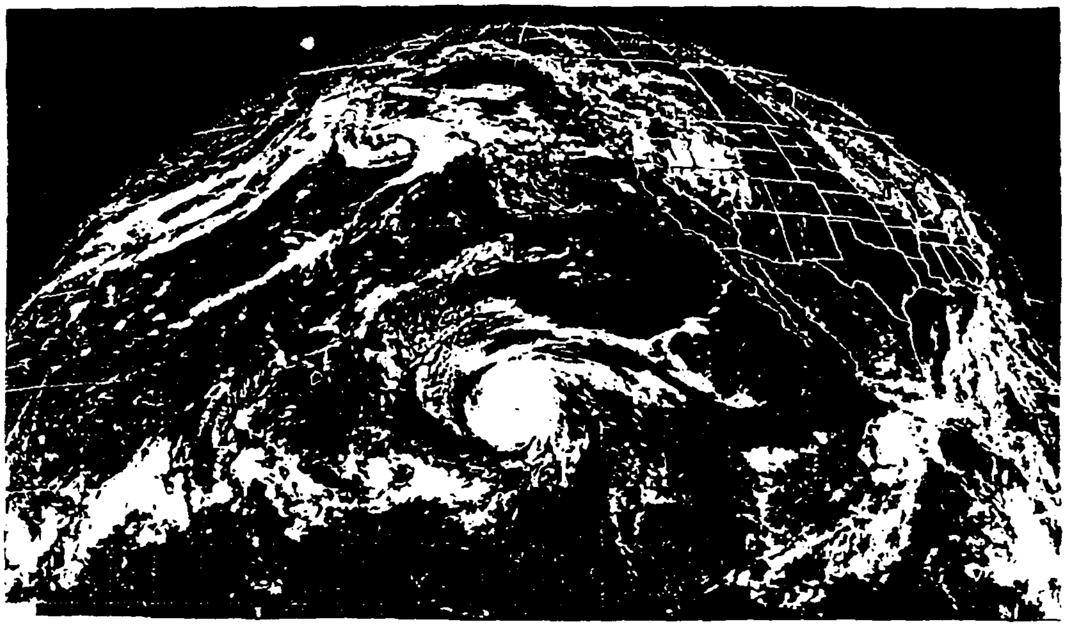

Figure 20. As in Fig. 1 except for Oct. 13, 1983 image.

Figure 21a. As in Fig. 2a except for original HSWO segmentation using image in Fig. 20.

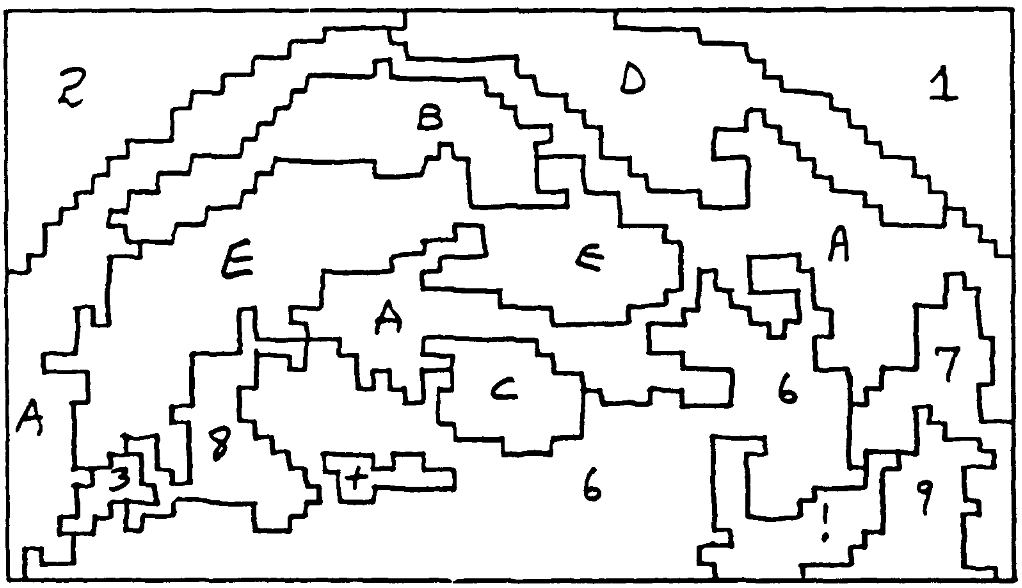

Figure 21b. As in Fig. 2b except for original HSWO segmentation using image in Fig. 20.

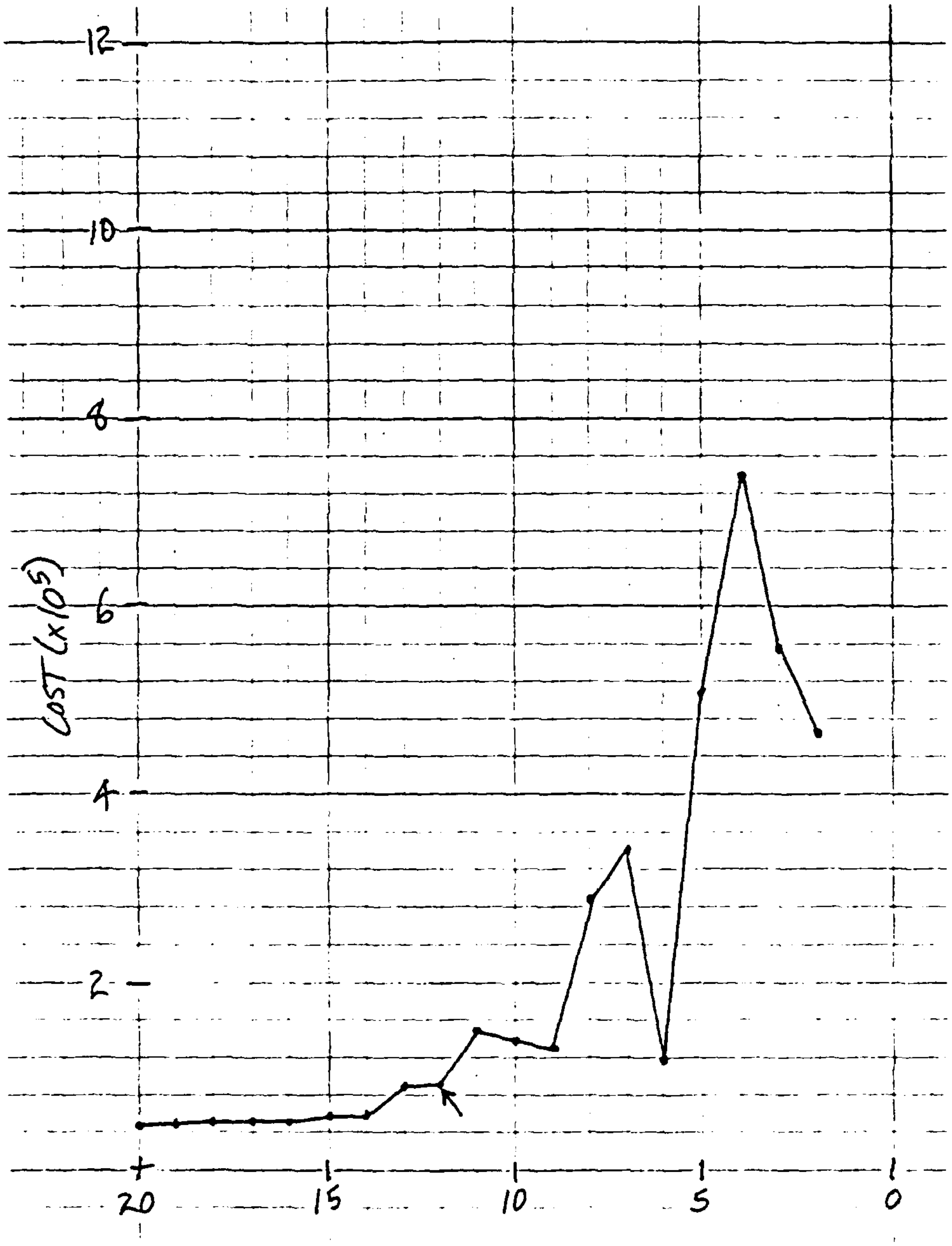

Figure 21c. As in Fig. 2c except for original HSWO segmentation using image in Fig. 20.

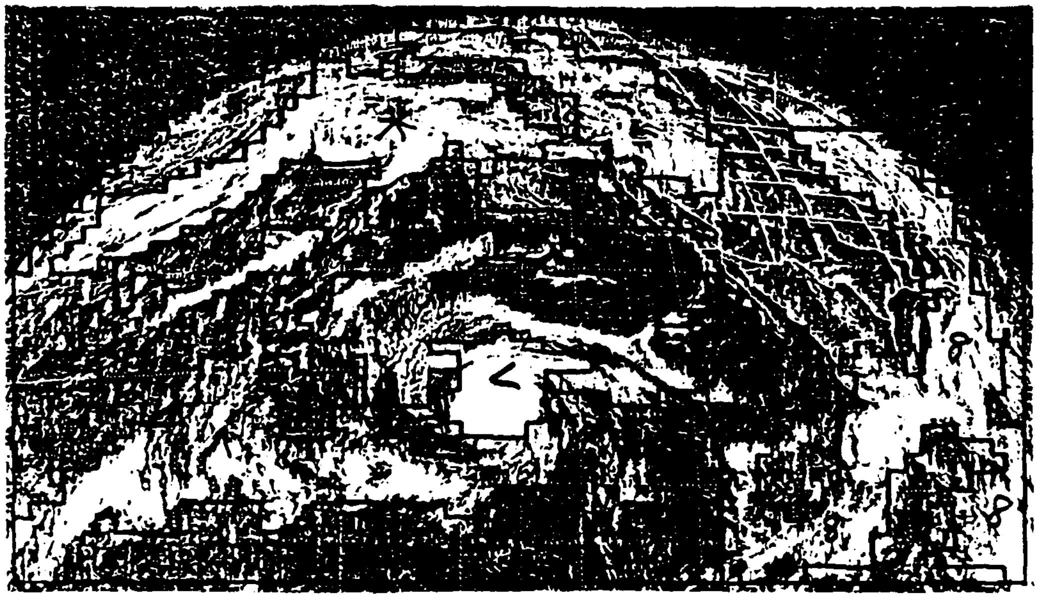

Figure 22a. As in Fig. 2a except for HSWO segmentation on image in Fig. 20 using cost function in Eqn. (4).

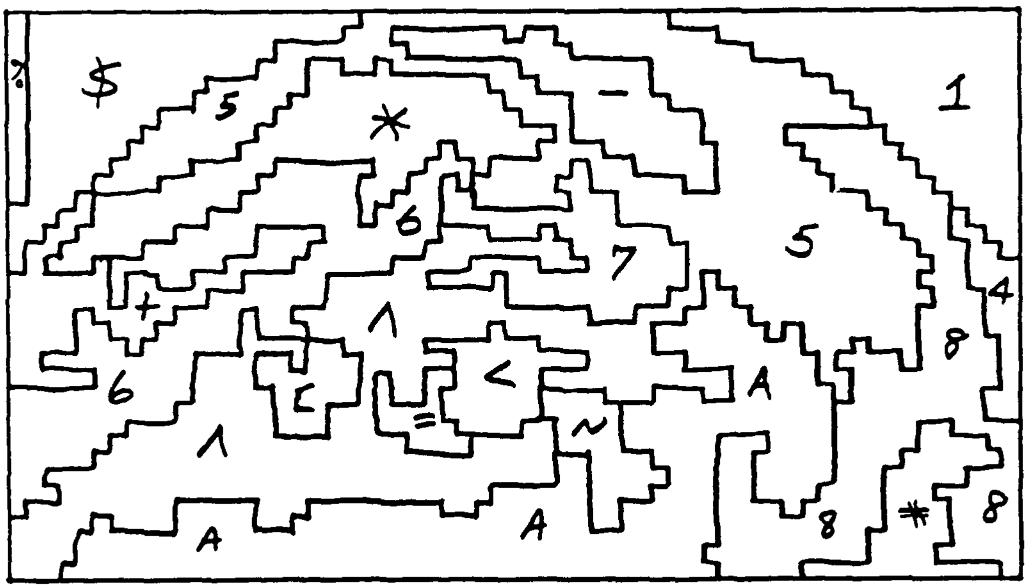

Figure 22b. As in Fig. 2b except for HSWO segmentation on image in Fig. 20 using cost function in Eqn. (4).

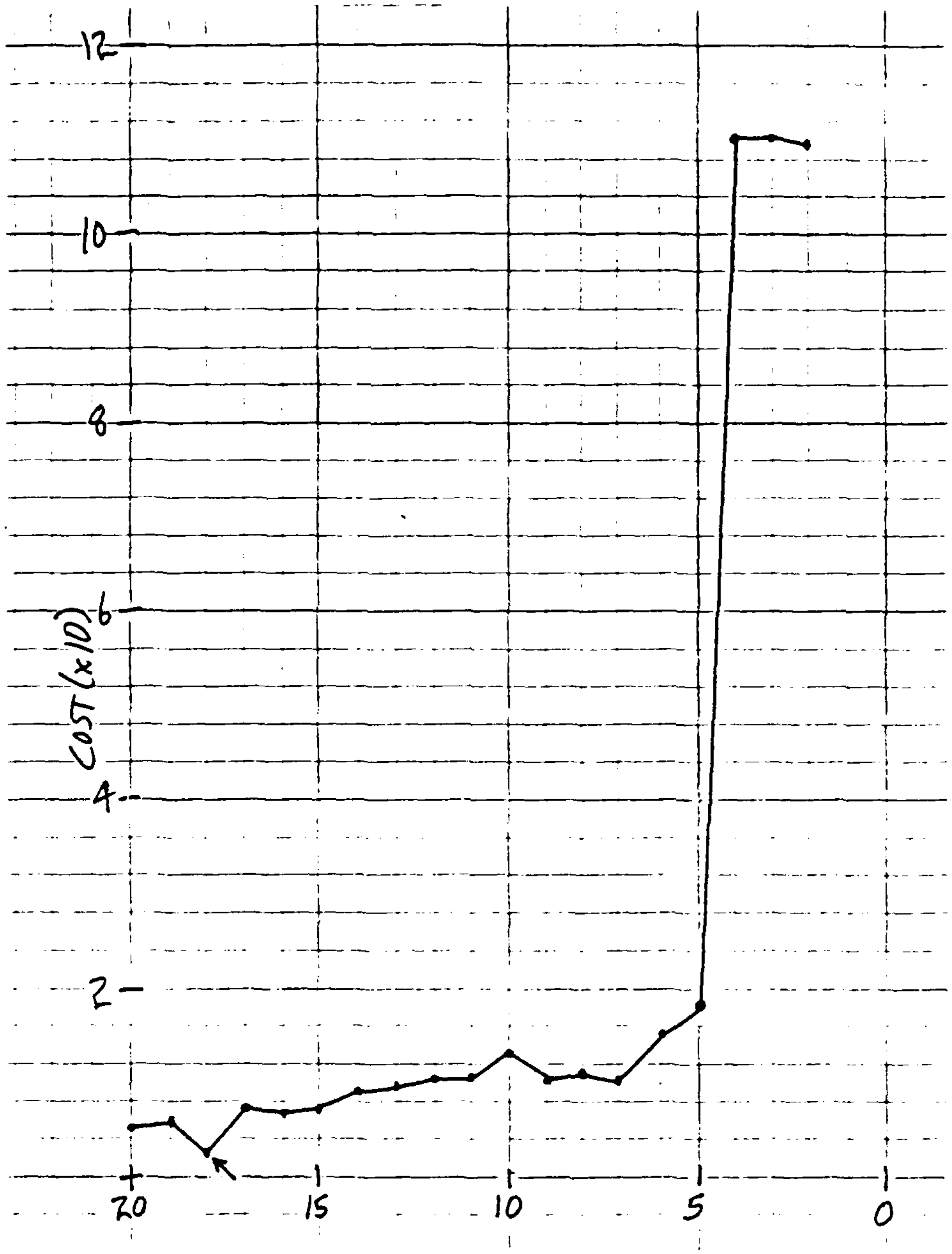

Figure 22c. As in Fig. 2c except for HSWO segmentation on image in Fig. 20 using cost function in Eqn. (4).

4.6 Oct. 16, 1983 Case

This, final case (Fig. 23) again has a standard front in the Bering Sea. There is an area of stratocumulus off of California and Baja. A tropical storm is located to the west as well as a hurricane off the Mexican coast.

The segmentation (Fig. 24) fails to resolve the cold front in this image because there is a broad region of bright, stratocumulus cells in the cold air behind the front. The tail of the front gets absorbed into this region (area A). The nature of these photographs is to have a generally brighter reflection along the planetary edges. The body of the front gets absorbed into this anomalous bright region (area C) that extends across the top of the image and even down into the tropics. The stratocumulus off of California is segmented well (area #), as are the tropical cyclones (areas ^ and *). Only a small part of the western (area 8) and eastern (area $) ITCZ is resolved.

The modified HSWO (Fig. 25) falls victim to the same circumstances regarding the front. The tail of the front combines with background area D and the head with the edge-effect area C. Even the tropical cyclones are absorbed into area C. The western ITCZ (area =) is segmented well, but the eastern ITCZ is lost.

4.7 Discussion

Upon examination of these six cases, the HSWO tests on the Nov. 15 case appear to have been deceptively good. The image at hand had well-defined regions that were easily distinguished from the background and from each other. The six cases presented here show the more typical nature of the imagery to be proc-

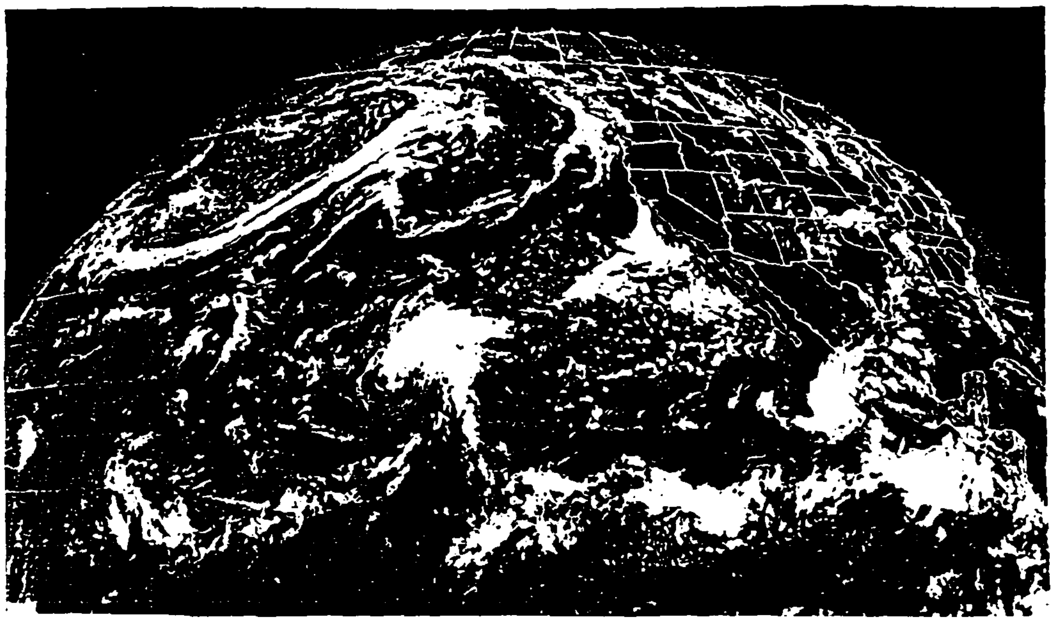

Figure 23. As in Fig. 1 except for Oct. 16, 1983 image.

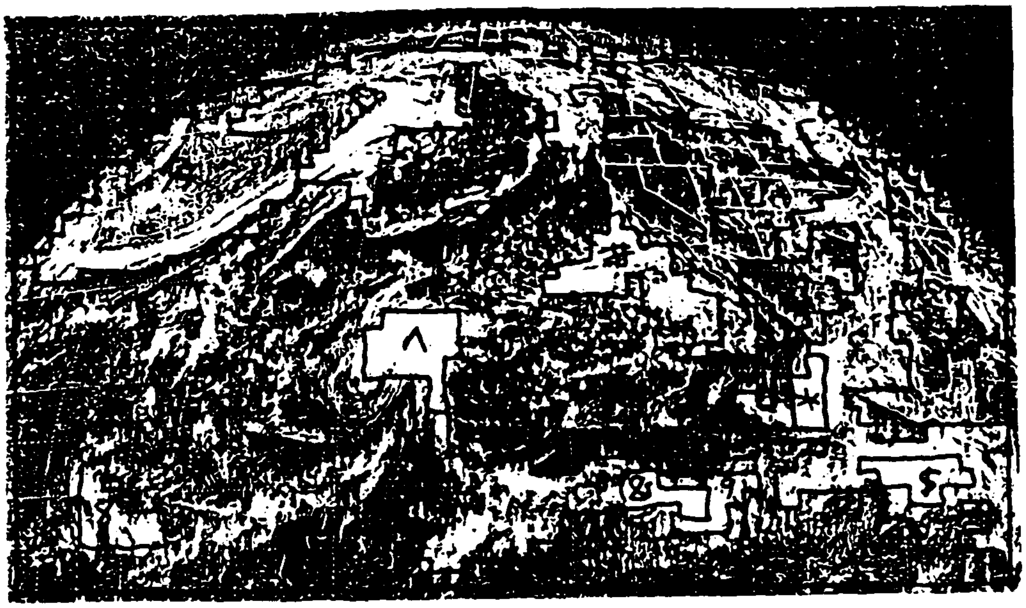

Figure 24a. As in Fig. 2a except for original HSWO segmentation using image in Fig. 23.

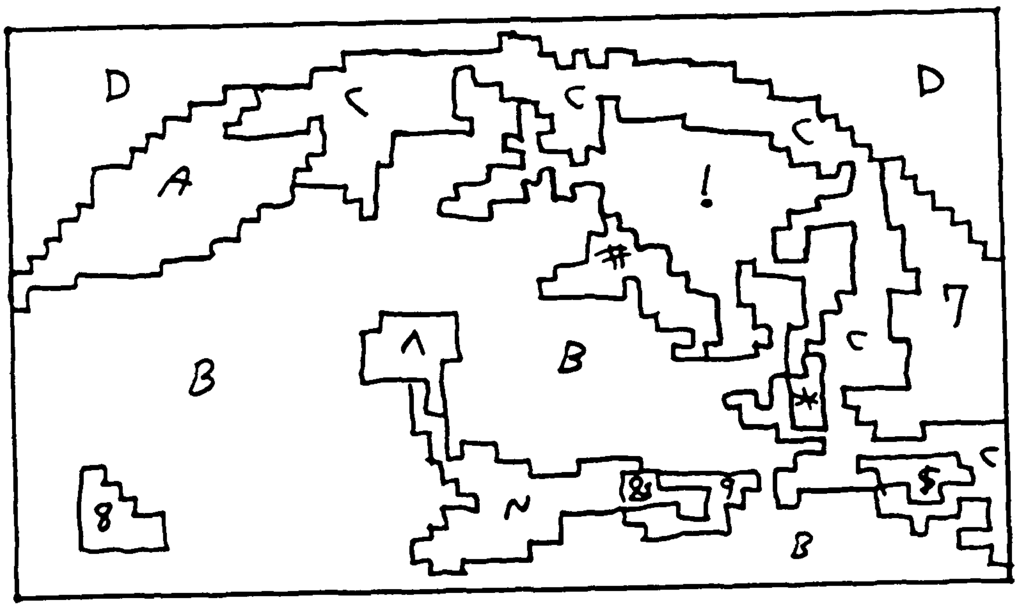

Figure 24b. As in Fig. 2b except for original HSWO segmentation using image in Fig. 23.

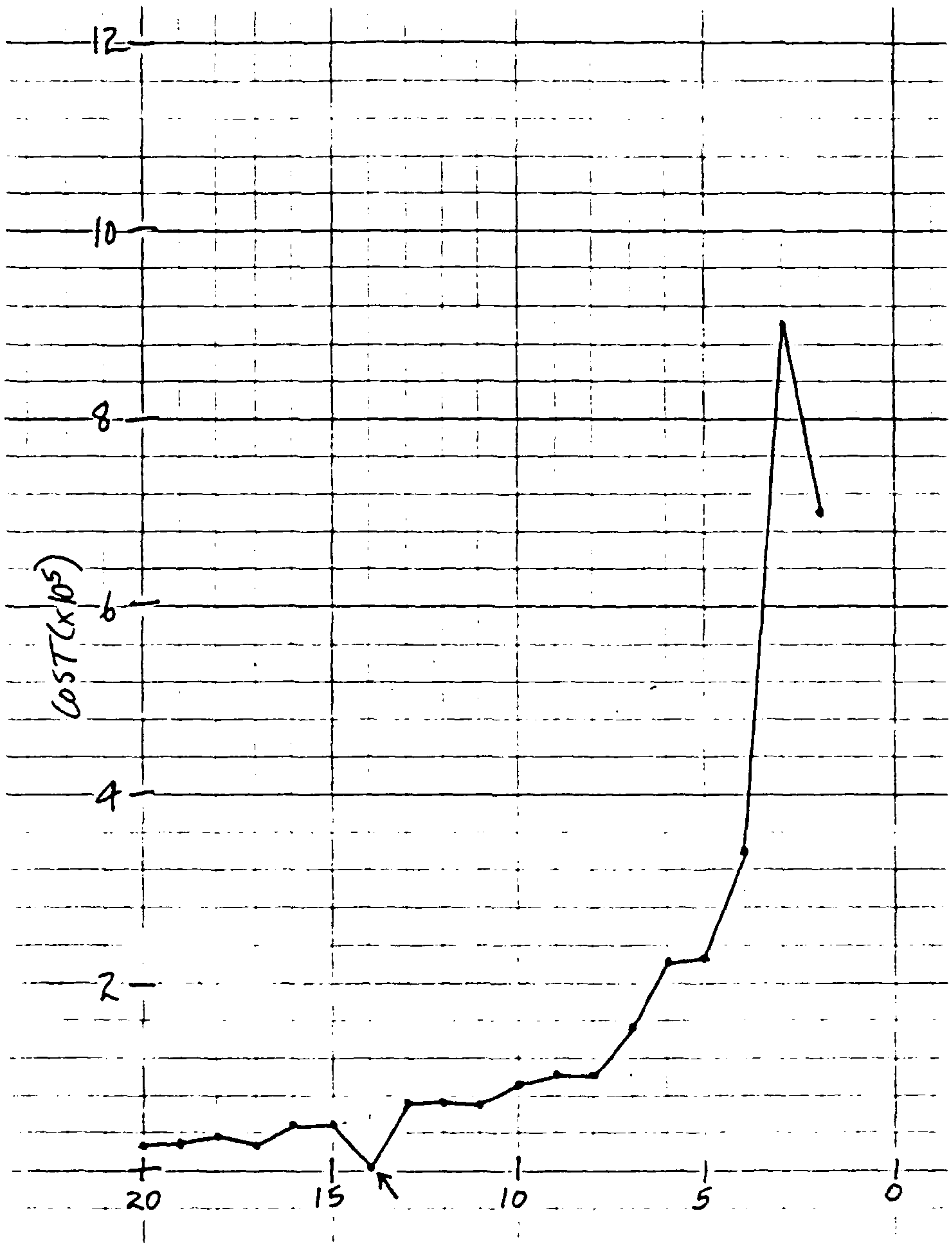

Figure 24c. As in Fig. 2c except for original HSWO segmentation using image in Fig. 23.

Figure 25a. As in Fig. 2a except for HSWO segmentation on image in Fig. 23 using cost function in Eqn. (4).

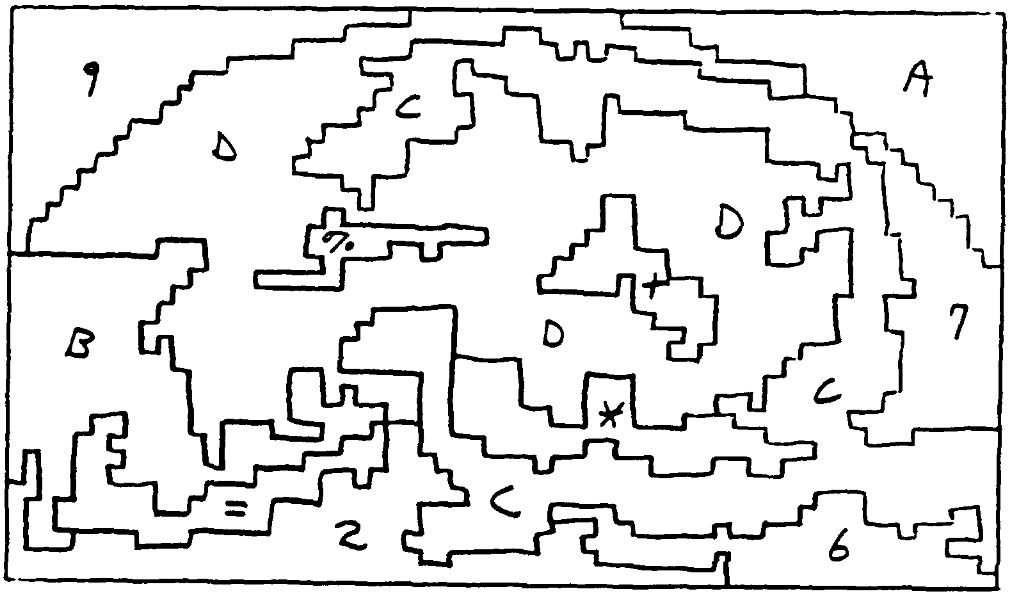

Figure 25b. As in Fig. 2b except for HSWO segmentation on image in Fig. 23 using cost function in Eqn. (4).

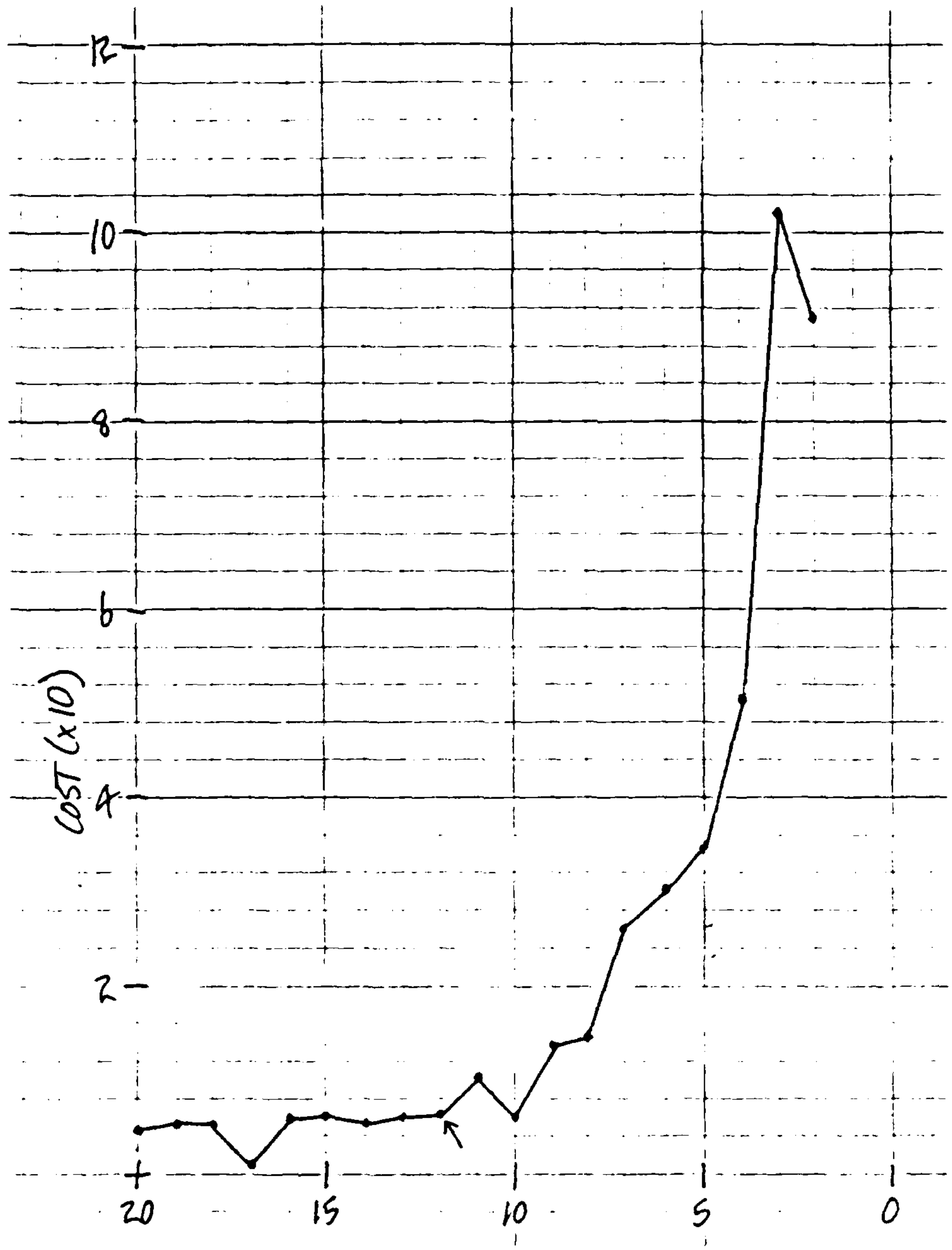

Figure 25c. As in Fig. 2c except for HSWO segmentation on image in Fig. 23 using cost function in Eqn. (4).

essed. The cloudy areas can be quite complex, and it takes considerable skill to be able to isolate the meaningful regions. HSWO alone is not capable of doing this task.

It may be possible to improve the HSWO segmentations by post-processing the initial regions. Perhaps a rule-based system or a neural net could specify which regions are correctly-segmented cloud features and which need to be segmented further or combined together.

Alternately, a different segmentation approach might be devised which applies constraints on the region-growing process. In other words, as the areas are considered for combination, the method would consider whether the resulting region makes sense in terms of its shape and its context in the emerging scene. Such a methodology would require fairly basic research in image segmentation theory. However, it seems clear that the meteorological features that must be isolated depend on more than simple bright vs. dark considerations. In particular, it would be interesting to apply the so-called Boltzmann machine neural network methodology to this problem.

The experiments conducted here have been conducted on digitized, photographic images. It may be that the use of original satellite data would produce better results. NOARL has a number of mosaiced DMSP images that might be tried, as well as some fairly wide-view AVHRR data. It may be useful to try HSWO on these cases.

There are other region-growing methods in the literature besides HSWO. It may be illuminating to conduct a literature search of other image segmentation methods.

Finally, it may be that the segmentation is such an integral part of the feature classification process that it simply cannot be done as a single step. Perhaps one could isolate the easily-discernible features, and then proceed as does the SIAMES expert system. Using constraints and partial knowledge, one could begin an intelligent search of the remaining image for other features of interest. Such a top-down approach combined with partial, bottom-up information might work.

5. Conclusions

In this paper, the Hierarchical Stepwise Optimization algorithm is applied to the problem of segmenting cloud features in satellite images. Various forms of the cost function have been explored as potential ways to improve the segmentations. In tests on the Nov. 15, 1983 image, the form given in Eqn. (4) proved to be superior.

The original HSWO and the modified version have been tested on six images. Although both forms of the algorithm show promise in the ability to segment certain cloud features, the scheme is quite inadequate in discriminating many of the complex cloud patterns that appear in these images. A certain amount of the problem may result from the use of data digitized from photographs. However, it appears likely that the very nature of the types of cloud features of interest would thwart attempts to provide a segmentation based only on bright vs. dark considerations.

It is recommended that a new approach be devised that takes into account some top-level information about large-scale cloud features. Constraints on the size and shape of features allowed, and on the spatial interrelations of such features, should be included in the segmentation scheme. For example, we know that the ITCZ has a preferred location in the tropics and that it tends to span the width of the image. Similarly, frontal bands tend to be located and oriented in certain ways. Segmentation into the more likely cloud configurations would be given preference over segmentations that do not fit the expected model as well.

The neural network methodology known as the "Boltzman Machine" is a constraint-satisfaction methodology. These networks are useful in solving problems that must satisfy many constraints, some of which may even be contradictory. This methodology should be explored to see whether the segmentation problem could be defined in a form that it could solve. Additionally, the literature should be scanned to see whether there are any other approaches that may be applicable to the cloud feature segmentation problem.

REFERENCES

Beaulieu, J.-M. and M. Goldberg, 1989: Hierarchy in picture segmentation - a stepwise optimization approach. IEEE Trans. on Patt. Anal. and Machine Intell., 11, 2 pp 150-163.

Peak, J.E., 1991a: Neural Network Methodologies and their Potential Application to Cloud Pattern Recognition. NOARL Technical Note 103, Naval Oceanographic and Atmospheric Research Laboratory, Atmospheric Directorate, Monterey, CA 93943-5006. 52 pp.

______, 1991b: Application of Neural Networks to Large-Scale Cloud Pattern Recognition - Further Experiments. NOARL Technical Note 104, Naval Oceanographic and Atmospheric Research Laboratory, Atmospheric Directorate, Monterey, CA 93943-5006. 45 pp.

DISTRIBUTION LIST

SPAWARSYSCOM
ATTN: PMW-141
WASHINGTON, DC 20363-5100

NOARL (10)
ATTN: CODE 125L
JCSSC, MS 39529-5004

NOARL
ATTN: CODE 125P
JCSSC, MS 39529-5004

NOARL
ATTN: CODE 300
JCSSC, MS 39529-5004

OFFICE OF NAVAL RESEARCH
ATTN: CODE 10
800 N. QUINCY ST.
ARLINGTON, VA 22217-5000

WOODS HOLE OCEANOGRAPHIC INST.
ATTN: AI APPLICATIONS
P.O. BOX 32
WOODS HOLE, MA 02543

SCRIPOPS INST. OF OCEANOGRAPHY
ATTN: AI APPLICATIONS
BOX 6049
SAN DIEGO, CA 92106

OFFICE OF NAVAL TECHNOLOGY
ATTN: DR. P. SELWYN, CODE 20
800 N. QUINCY ST.
ARLINGTON, VA 22217-5000

OFFICE OF NAVAL TECHNOLOGY
DR. M. BRISCOE, CODE 228
800 N. QUINCY ST.
ARLINGTON, VA 22217-5000

OFFICE OF NAVAL RESEARCH
ATTN: CODE 12
800 N. QUINCY ST.
ARLINGTON, VA 22217-5000

OFFICE OF NAVAL RESEARCH
ATTN: HEAD, OCEAN SCIENCES DIV
CODE 1122
ARLINGTON, VA 22217-5000

U.S. NAVAL ACADEMY
ATTN: LIBRARY REPORTS
ANNAPOLIS, MD 21402

U.S. NAVAL ACADEMY
ATTN: OCEANOGRAPHY DEPT.
ANNAPOLIS, MD 21402

NAVAL POSTGRADUATE SCHOOL
ATTN: CODE MR
MONTEREY, CA 93943-5000

NAVAL POSTGRADUATE SCHOOL
ATTN: 0142
MONTEREY, CA 93943-5002

SPAWARSYSCOM
ATTN: CODE 312
NAT. CTR. #1
WASHINGTON, DC 20363-5100

SPAWARSYSCOM
ATTN: CODE PMW-141
NAT. CTR. #1
WASHINGTON, DC 20363-5100

NAVOCEANSYSCEN
ATTN: J. RICHTER, CODE 54
SAN DIEGO, CA 92152-5000

PACMISTESTCEN
ATTN: GEOPHYSICS OFFICER
PT. MUGU, CA 93042

AFGWC/DAPL
ATTN: TECH. LIBRARY
OFFUTT AFB, NE 68113

AFGL/LY
ATTN: MET. OFFICER
HANSCOM AFB, MA 01731

COMMANDER/DIRECTOR
ASL, WHITE SANDS
ATTN: SLCAS-AE
WSMR, NM 88002-5501

NOAA-NESDIS LIAISON
ATTN: CODE SC2
NASA-JOHNSON SPACE CENTER
HOUSTON, TX 77058

DIRECTOR
NATIONAL EARTH SAT. SERV/SEL
ATTN: FB-4, S321B
SUITLAND, MD 20233

FEDERAL COORD. FOR METEORO.
SERVS. & SUP. RSCH. (OFCM)
ATTN: OPERATIONS SECTION
11426 ROCKVILLE PIKE
ROCKVILLE, MD 20852

DIRECTOR, NOAA
ATTN: TECH. DEVELOPMENT LAB
GRAMAX BLDG.
8060 13TH ST.
SILVER SPRING, MD 20910

NCAR
ATTN: LIBRARY ACQUISITIONS
P.O. BOX 3000
BOULDER, CO 80307

NATIONAL SCIENCE FOUNDATION
ATTN: ATMOS. SCIENCES DIV.
1800 G STREET, NW
WASHINGTON, DC 20550

SCRIPPS INSTITUTION OF
OCEANOGRAPHY, LIBRARY
ATTN: DOCUMENTS/REPORTS SECT.
LA JOLLA, CA 92037

WOODS HOLE OCEANO. INST.
ATTN: DOCUMENT LIBRARY LO-206
WOODS HOLE, MA 02543

COLORADO STATE UNIVERSITY
ATTN: ATMOS. SCIENCES DEPT
ATTN: LIBRARIAN
FT. COLLINS, CO 80523

UNIVERSITY OF WASHINGTON
ATTN: ATMOS. SCIENCES DEPT.
SEATTLE, WA 98195

PENNSYLVANIA STATE UNIV.
ATTN: METEOROLOGY DEPT.
503 DEIKE BLDG.
UNIVERSITY PARK, PA 16802

AMERICAN METEORO. SOCIETY
ATTN: METEOR. & GEOASTRO. ABST
P.O. BOX 1736
WASHINGTON, DC 20013

REPORT DOCUMENTATION PAGE

Form Approved
OMB No. 0704-0188

1. Agency Use Only *(Leave blank).*

2. Report Date. March 1991

3. Report Type and Dates Covered. Final

4. Title and Subtitle.
Use of Hierarchical Stepwise Optimization for the Segmentation of Cloud Features

5. Funding Numbers.
Program Element No. 62435N
Project No. RM35G82
Task No. 4
Accession No. DN651750

6. Author(s).
J.E. Peak

7. Performing Organization Name(s) and Address(es).
Computer Sciences Corporation, Monterey, CA 93943-5006

Naval Oceanographic and Atmospheric Research Laboratory
Atmospheric Directorate, Attn Dr. P. Tag
Monterey, CA 93943-5006

8. Performing Organization Report Number.
NOARL Technical Note 106

9. Sponsoring/Monitoring Agency Name(s) and Address(es).
Office of Naval Research (ONT)
800 N. Quincy St.
Arlington, VA 22217-5000

10. Sponsoring/Monitoring Agency Report Number.
NOARL Technical Note 106

11. Supplementary Notes.

12a. Distribution/Availability Statement.
Approved for public release; distribution is unlimited.

12b. Distribution Code.

13. Abstract *(Maximum 200 words).*

The Hierarchical Stepwise Optimization algorithm of Beaulieu and Goldberg (1989) is applied to the segmentation of satellite images into meaningful, large-scale cloud features. GOES-W visible imagery is used. Several different forms of the cost function are explored in an attempt to improve the segmentation of the Nov. 15, 1983 case. A new cost function is shown to result in a superior segmentation. Both HSWO versions are tested on six additional cases. A modification to the HSWO approach is suggested for further research.

14. Subject Terms.
AI
Artificial intelligence
Satellite imagery
Pattern recognition
Segmentation

15. Number of Pages. 71

16. Price Code.

17. Security Classification of Report.	18. Security Classification of This Page.	19. Security Classification of Abstract.	20. Limitation of Abstract.
UNCLASSIFIED	UNCLASSIFIED	UNCLASSIFIED	Same as report

NSN 7540-01-280-5500

Standard Form 298 (Rev 2-89)
Prescribed by ANSI Std Z39-18
298-102